AIR POLLUTION EFFECTS ON THE FAÇADE OF THE BOTTER APARTMENT IN ISTANBUL

A Thesis Submitted to
the Graduate School of Engineering and Sciences of
Izmir Institute of Technology
in Partial Fulfillment of the Requirements for the Degree of

MASTER OF SCIENCE

In Architectural Restoration

by
Birsen PARLAK

July 2010
İZMİR

We approve the thesis of **Birsen PARLAK**

_____

Prof. Dr. Hasan BÖKE
Supervisor

_____

Prof. Dr. Başak İPEKOĞLU
Committee Member

_____

Assoc. Prof. Dr. Aysun SOFUOĞLU
Committee Member

05 July 2010

_____

Prof. Dr. Başak İPEKOĞLU
Head of the Department of
Architectural Restoration

_____

Assoc. Prof. Dr. Talat YALÇIN
Dean of the Graduate School of
Engineering and Sciences

ACKNOWLEDGEMENTS

This study would not have been possible without the support, encouragement and love of many people.

I am indebted to my supervisor Prof. Dr. Hasan Böke for his valuable contributions, continuous support and encouragement throughout the period of this thesis.

I would like to thank the jury members Prof. Dr. Başak İpekoğlu and Assoc. Prof. Dr. Aysun Sofuoğlu for accepting to attend my thesis defence seminar and their valuable suggestions.

I would like to express my thanks to the staff of the Centre for the Materials Research of the Institute for SEM-EDS, XRD and TGA analyses. I would also thank Spec. Kerim Şerifaki and Elif Uğurlu and Res. Assist. Fulya Murtezaoğlu and Çağlayan Deniz Kaplan for their help during the laboratory studies in Material Conservation Laboratory.

I would like to express my thanks to Prof. Dr. Afife Batur and Ayşe Akyıl Kantarcıoğlu for sharing their achieves.

I would like to express my special thanks to my dear friends Gizem Çıtak, Serap Demir and Ayşe Nur Şenel for their friendship and moral support. I am grateful to my special friend Emrah İncel for his support and love.

Finally, I am indebted to my mother Kafiye Parlak, my father Ali Parlak, my brother Ersan Parlak and my sister Fatmagül Parlak for their patience, endless love and encouragements during this study. This thesis is dedicated to them.

ABSTRACT

AIR POLLUTION EFFECTS ON THE FACADE OF THE BOTTER APARTMENT IN ISTANBUL

Air pollution showed a large increase with the rapid development of industry in the middle of the 18th century. Air pollution has been affecting cultural heritage along with human health. Limestone is one of the most affected building materials from the air pollution. Carbon, sulphure and nitrogen gases are the main components which are affective in the deterioration of limestone and their rate increased with air pollution. Sulphure dioxide (SO_2) reacts with the calcite crystals ($CaCO_3$) that are the main structure of limestone and leads to the formation of gypsum ($CaSO_4.2H_2O$).

In this study, the formation of gypsum on limestone was investigated on the façade of the Botter Apartment within the restoration and conservation studies. For this purpose physical, mineralogical and chemical compositions of weathered limestone were determined by XRD, SEM-EDS, FT-IR and TGA analyses. The weathering forms caused by air pollution were documented with drawing (mapping) and photographs of front façade of Botter Apartment.

The results of the study indicated that gypsum formation on limestone surfaces is mainly originated from wet and dry deposition process of sulphur dioxide. Condensation may also play an important role in gypsum formation on such sheltered surfaces in addition to dry deposition. On sheltered surfaces of limestone, due to the dry deposition of gypsum formation proceeds as black crust formation. The gypsum formation has not restricted on the surface of limestone. Deeper penetration and absorption of sulphure dioxide are observed in limestone because of their more porous structure.

In Istanbul average daily temperature is low and average relative humidity and sulphure dioxide concentrations are high in winter time. The results of this study indicated that İstanbul atmosphere, with its coinciding high relative humidity and high sulphure dioxide concentrations in winter have led to gypsum formation on limestone. This situation has been encountered in all calcareous stones used in the construction of the buildings.

ÖZET

HAVA KİRLİLİĞİNİN İSTANBUL'DA BULUNAN BOTTER APARTMANININ CEPHESİNE OLAN ETKİLERİ

Hava kirliliği, 18. yy ın ortalarında endüstrinin hızlı şekilde gelişmesiyle birlikte büyük bir artış göstermiştir. Hava kirliliğinde meydana gelen bu artış insan sağlığının yanında kültürel mirasımız olan tarihi yapıları da olumsuz yönde etkilemektedir. Kireç taşları da hava kirliliğinden en fazla etkilenen yapı elemeanlarından birisidir. Karbon, kükürt ve nitrojen dioksit gazları kireç taşlarının bozulmasında etkili olan başlıca gazlardır. Hava kirliliğiyle birlikte oranları artan sülfür dioksit (SO_2) gazı kireç taşının ana yapısını oluşturan kalsit kristalleri ($CaCO_3$) ile tepkimeye girerek alçı taşı ($CaSO_4.2H_2O$) oluşumuna neden olmaktadır.

Bu çalışmada Botter Apartmanının restorasyon ve koruma çalışmaları kapsamında cephedeki kireçtaşlarının üzerinde oluşan alçı oluşumu incelenmiştir. Bu amaçla; hava kirliliğinden etkilenmiş kireçtaşlarının fiziksel, kimyasal ve mineralojik özellikleri XRD, SEM-EDS, FT-IR ve TGA analizleri ile belirlenmiştir. Apartmanın ön cephesindeki hava kirliliğine bağlı bozulmalar çizim ve fotoğraflarla belgelenmiştir.

Çalışmanın sonuçları göstermiştir ki, kireçtaşı yüzeylerindeki alçıtaşı oluşumu genellikle sülfür dioksidin ıslak ve kuru depolanmasından kaynaklanır. Korunaklı yüzeylerdeki yoğunlaşma da alçı oluşumunda kuru depolanma gibi önemli bir rol oynar. Kireçtaşının korunaklı yüzeylerinde alçı oluşumu kuru depolanmaya bağlı olarak siyah kabuk oluşumu şeklinde ilerler. Alçı oluşumu kireçtaşı yüzeyiyle sınırlı değildir. Kireçtaşlarının daha gözenekli yapısı nedeniyle kükürt dioksit emilimi ve içerilere nüfus ettiği gözlenmektedir.

İstanbulda kış aylarında günlük ortalama sıcaklıkları düşük, ortalama bağıl nem ve SO_2 konsantrasyonları yüksektir. Bu çalışmanın sonuçlarına göre, yüksek bağıl nem ve SO_2 konsantrasyonuyla İstanbul atmosferi, kireç taşlarında alçı oluşumuna neden olan koşullara sahiptir. Bu durum, aynı zamanda bina yapımında kullanılan bütün kalkerli taşları için de geçerlidir.

TABLE OF CONTENTS

LIST OF FIGURES viii

LIST OF TABLES xi

CHAPTER 1. INTRODUCTION 1

1.1. Historical and Architectural Characteristics of Botter Apartment 2

1.2. Stones Used in the Construction of Façade of Botter Apartment 12

1.3. Air Pollution and Climatic Conditions in İstanbul 12

1.4. Effects of Air Pollution on Limestone 18

1.5. Protection of Calcareous Stones From the Air Pollution 25

1.6. Aim of Study 26

CHAPTER 2. EXPERIMENTAL METHODS 28

2.1. Site Survey 28

2.2. Sampling 28

2.3. Experimental Study 32

2.3.1. Determination of Basic Physical Properties of Limestone 32

2.3.2. Determination of Mineralogical Compositions of Limestone 33

2.3.3. Determination of Chemical Compositions and Microstructural Properties of Limestone 33

2.3.4. Determination of Weight Loss of Limestone by Thermogravimetric Analysis 33

CHAPTER 3. RESULTS AND DISCUSSION 34

3.1. Visual Analysis of Weathering Forms Observed on the Façade of the Botter Apartment 34

3.2. Basic Properties of Limestone 40

3.3. Mineralogical Compositions of Limestone Samples 42

3.3.1. Mineralogical Compositions of Unweathered Limestone 42

3.3.2. Mineralogical Compositions of Limestone Affected from Air Pollution 46

3.4. Chemical Compositions of Unweathered and Weathered Samples 52
3.5. Determination of Weight Loss of Samples by Thermogravimetric Analysis 61

CHAPTER 4. CONCLUSION 66

REFERENCES 68

LIST OF FIGURES

Figure **Page**

Figure 1.Aerial photo showing the location of the plot of Botter Apartment on İstiklal Avenue 2

Figure 2. Plan D'assurances of Beyoğlu (Sigorta Planı) drawn by Jacques Pervititch in 1932 3

Figure 3. Façade of İstiklal Avenue 4

Figure 4 Measured façade drawing of the Botter Apartment 6

Figure 5. Florally ornamented main entrance door of Botter Apartment 7

Figure 6. Original elevator of Botter Apartment 8

Figure 7. Original watercolor painting of D'Aronco showing the atelier and main entrance door 9

Figure 8. Original watercolor paintings of D'Aronco showing the terrace and fifth floor façade ornamentations 10

Figure 9. Original watercolor paintings of D'Aronco 10

Figure 10. Detail from the terrace floor of the Apartment at 1980s 11

Figure 11. Detail from the terrace floor of the Apartment at 2009 11

Figure 12.Monthly SO_2 concentrations in Beşiktaş - Istanbul between the years 2004 – 2009 14

Figure 13.Monthly concentrations of Particulate Matters less than 10 µm in Beşiktaş - Istanbul between the years 2004 – 2009 15

Figure 14.Monthly average values of temperature and relative humidity between the years 2000 and 2009. 16

Figure 15.Monthly average values of rainfall between the years 2000 and 2009. 17

Figure 16.Monthly average values of wind speed between the years 2000 and 2009. 17

Figure 17. Gypsum formation on the stone surface by dry deposition of SO_2 19

Figure 18. Gypsum formation on the stone surface by wet deposition of SO_2 20

Figure 19. Schematic view of the layers 29

Figure 20. Façade of the Botter Apartment showing the places of samples taken from 30

Figure 21. Figure showing the place of Roof Floor Sample (RFS) taken from. 31

Figure 22. Figure showing the place of Fifth Floor Sample (FfFS) taken from. 31

Figure 23. Figure showing the place of First Floor Sample (FsFS) taken from. 31

Figure 24.Mapping of weathering forms observed on the façade of Botter Apartment. 35
Figure 25. Break out on the façade of the Botter Apartment..... 36
Figure 26. Back weeathering due to the loss of black crust 37
Figure 27. Coloration due to the corrosion products of the metals..... 37
Figure 28. Microbiological Colonization on the façade of the Botter Apartment..... 37
Figure 29. Black Crust on the façade of the Botter Apartment 38
Figure 30. Higher Plants on the façade of the Botter Apartment 38
Figure 31. Scaling on the façade of the Botter Apartment 39
Figure 32. Present condition of the Botter Apartment..... 39
Figure 33. SEM images of limestone showing calcite minerals, the sea shell and corals in composition with a magnification setting of (a) and (b) 130 x, (c) 250 x and (d) 350 x and accelerating voltage 15 kV 40
Figure 34. Porosity values of the FsFS from surface to the inner. 41
Figure 35. Porosity values of the RFS from surface to the inner..... 42
Figure 36. XRD patterns of the Unweathered Layer of the samples (a): Roof Floor Sample (RFS-UW), (b): Fifth Floor Sample (FfFS-UW), (c): First Floor Sample (FsFS-UW)..... 43
Figure 37. FT-IR graphs of Unweathered Layer of the samples (a): Roof Floor Sample (RFS-UW), (b): Fifth Floor Sample (FfFS-UW), (c): First Floor Sample (FsFS-UW)..... 44
Figure 38. XRD patterns of the Weathered Layers (from surface to 5mm inner) of the samples (a): Roof Floor Sample (RFS-W1), (b): Fifth Floor Sample (FfFS-W1), (c): First Floor Sample (FsFS-W1) 46
Figure 39. XRD patterns of the Weathered Layer-2 (approximately from 5mm to 15 mm inside) of the samples (a): Roof Floor Sample (RFS-W2), (b): Fifth Floor Sample (FfFS-W2), (c): First Floor Sample (FsFS-W2)..... 48
Figure 40. FT-IR graphs of the Weathered Layer-1 of the samples (A): Roof Floor Sample (RFS-W1), (B): Fifth Floor Sample (FfFS-W1), (C): First Floor Sample (FsFS-W1)..... 49
Figure 41. FT-IR graphs of the Weathered Layer-2 (approximately from 5mm to 15 mm inside) of the samples (A): Roof Floor Sample (RFS-W2), (B): Fifth Floor Sample (FfFS-W2), (C): First Floor Sample (FsFS-W2)..... 51

Figure 42. EDX spectrum and chemical compositions of the First Floor Sample (a): Unweathered Layer, (b): Weathered Layer-1, (c): Weathered Layer-2 with matrix 256X200 53
Figure 43. Gypsum rates of the FsFS from surface to the 9,8 mm inside. 54
Figure 44. SE image of the FsFS from surface to the 2,2 mm inside showing the gypsum formation. 55
Figure 45. SE image and EDX spectrum of the gypsum crystals on the Roof Floor sample (RFS) with a magnification setting of 1500x and accelerating voltage 5 kV 56
Figure 46. % Ca value from surface to the 9.8 mm inner in the sample of First Floor (FsFS)..... 57
Figure 47. SEM images of gypsum crystals at Roof Floor Sample (RFS) with a magnification setting of (a) 5000 x, (b) 2500 x, (c) 10000 x and (d) 20000 x and accelerating voltage 5 kV..... 58
Figure 48. % S value from surface to the 9.8 mm inner in the sample of First Floor (FsFS)..... 59
Figure 49. % Na value from surface to the 9.8 mm inner in the sample of First Floor (FsFS)..... 59
Figure 50. % Cl value from surface to the 9.8 mm inner in the sample of First Floor (FsFS)..... 60
Figure 51. % Al value from surface to the 9.8 mm inner in the sample of First Floor (FsFS)..... 60
Figure 52. % Si value from surface to the 9.8 mm inner in the sample of First Floor (FsFS)..... 61
Figure 53. % Mg value from surface to the 9.8 mm inner in the sample of First Floor (FsFS)..... 61
Figure 54. TGA analysis of RFS-Weathered Layer-1 63
Figure 55. TGA analysis of RFS-Unweathered Layer 64
Figure 56. TGA analysis of FsFS- Weathered Layer-1 64
Figure 57. TGA analysis of FfFS- Weathered Layer-1 (the sample which taken from the unsheltered place) 65

LIST OF TABLES

Table **Page**

Table 1. Monthly SO_2 concentrations in Beşiktaş - Istanbul between the years 2004 – 2009 14

Table 2. Monthly concentrations of Particulate Matters less than 10 μm in Beşiktaş - Istanbul between the years 2004 – 2009 15

Table 3. List of samples 29

Table 4. Table showing the amount of the elements in Roof Floor Sample (RFS) 55

Table 5. TGA analysis showing the % weight loss of samples between the different range of temperatures 62

CHAPTER 1

INTRODUCTION

Historic monuments are the evidences of a particular civilization with their construction techniques, craftsmanship, materials, and traditions in addition to architectural work (Venice Charter 2009). The historic monuments are the living witnesses of their age-old traditions and they should be safeguarded for the future generations with the full richness of their authenticity (Venice Charter 2009).

The deterioration of historic buildings constructed by calcareous stones have been accelerated by the use of fossil fuel that resulted in the increase of sulphure dioxide (SO_2) concentration in the atmosphere. Limestone has been one of the most commonly used calcareous stones in the construction of the historic monuments in Turkey. Sulphure dioxide reacts with limestone composed mainly of calcite crystals ($CaCO_3$) and converts it into gypsum. Gypsum is very soluble and occupies more volume than $CaCO_3$. As a result, limestone is eroded and disintegrated (Gauri and Bandyopadhyay 1999).

Istanbul, an important city in historical respect being the capital of three important empires Roman, Byzantine and Ottoman, hosted many different civilizations and cultures. Limestone was the mostly used construction material of those civilizations. The historical buildings and monuments which are the witnesses of these civilizations are rapidly deteriorating by air pollution in Istanbul. The aim of this study is to investigate the effects of air pollution on historic buildings constructed with limestone.

In this study, deterioration problems of the façade of the Botter Apartment were investigated for the establishment of intervention criteria for its conservation works. The building was constructed in 1900-1901 by Raimondo D'Aronco as a workshop and residence for Jean Botter who was the personal tailor of Sultan Abdülhamid. This historical building gains importance in point of being the first example of Art Nouveau architecture built in Istanbul. Ornamented façade with the plant motif borders, female head and flowers are mostly affected parts from the air pollution by black crust formation.

Ornamentations also include the enlightening elements, stained glasses and metal moldings.

1.1. Historical and Architectural Characteristics of Botter Apartment

Botter Apartment with its original name Maison Botter located on the Istiklal Avenue near to the Tunnel Square in Beyoğlu, Istanbul (Figure 1, Figure 2). The plot on which the monument situated is narrow and deep. The location of the Apartment is on the northwest side of the plot. There is an annex at the southeast side of the plot.

Figure 1.Aerial photo showing the location of the plot of Botter Apartment on İstiklal Avenue (Source: Istanbul Büyükşehir Belediyesi 2010)

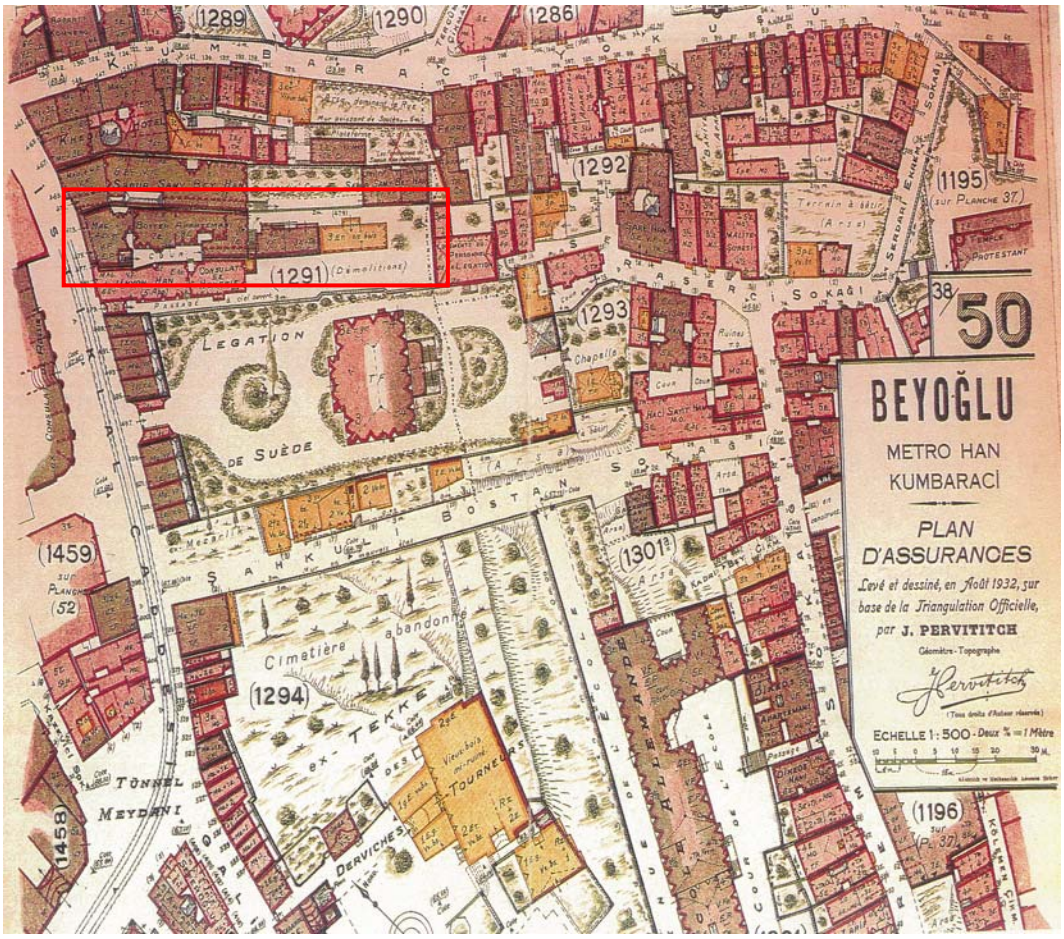

Figure 2. Plan D'assurances of Beyoğlu (Sigorta Planı) drawn by Jacques Pervititch in 1932 (Source: Afife Batur archieves)

Istiklal Avenue was known as Grande Rue de Pera (now İstiklal Caddesi) (Batur 1993). Istiklal Avenue was also called as Cadde-i Kebir (Grand Avenue) during the Ottoman period. It was a cosmopolitan avenue and was a popular spot for Ottoman intellectuals and European foreigners. Istiklal Avenue is surrounded by historical buildings (Figure 3) that reflects the architectural characteristics of their era, such as Flower Passage (Çiçek Pasajı), the Fish Market (Balık Pazarı), Galatasaray Lisesi, Mısır Apartment, Santa Maria and Saint Antonie Churches and consulates.

Botter Apartment is one of these important monuments located on the Istıklal Avenue. The monument is also important in respect of its being the first Art Nouveau styled building in İstanbul (Batur 1993).

Figure. 3. Façade of İstiklal Avenue (Source: Dökmeci and Çıracı 1990, Botter Apartment drawn by Birsen Parlak)

Art Nouveau movement, also entitled as 'New Art', was effective between the end of the 19th century and the beginning of the 20th century (Rona 1997). This movement began as a response to the monotony effects of the industrialization on art. There were two main concepts in art nouveau; floral and geometrical lines. Ferro banisters, balconies, stained glasses and the ornamented surfaces are the main characteristics of the era and geometrical and florally ornamentations (Rona 1997).

Botter Apartment was constructed in Art Nouveau style at the beginning of the twentieth century at the turbulent period of the empire (Batur 2005). This was a kind of way of dissipating its political power by constructing glorious palaces and buildings (Batur 2005). Famous architects from the Europe were calling and Raimondo D'Aronco was one of them.

Maison Botter was one of the most important buildings of the architect Raimondo D'Aronco. This monument was especially designed for Sultan Abdülhamid's tailor Jean Botter and built in 1900 in Istiklal Avenue (Batur 1993). Although the monument was known as an apartment, it was combined Jean Botter's atelier and the residence together. Apartment has seven stories; basement floor was used as a depot of the atelier. The measured drawing of the façade of the Botter apartment is shown in Figure 4.

The ground floor was used as a fashion house of Botter that was especially designed with high ceiling and mezzanine floor (Batur 1993). This was the prestige place of the Botter Fashion House with its decoration and curvilinear design. The first floor was used as an office by Jean Botter. The hall at the front façade was used as a guest room and the back rooms were used by the assistants of Botter. The upper three floors, setback storey and terrace floor were used as a residence by the Botter family.

İZMİR INSTITUTE OF TECHNOLOGY

THE GRADUATE SCHOOL OF ENGINEERING AND SCIENCES

A MASTER THESIS ON ARCHITECTURAL RESTORATION

AIR POLLUTION EFFECTS ON THE FAÇADE OF THE BOTTER APARTMENT IN İSTANBUL

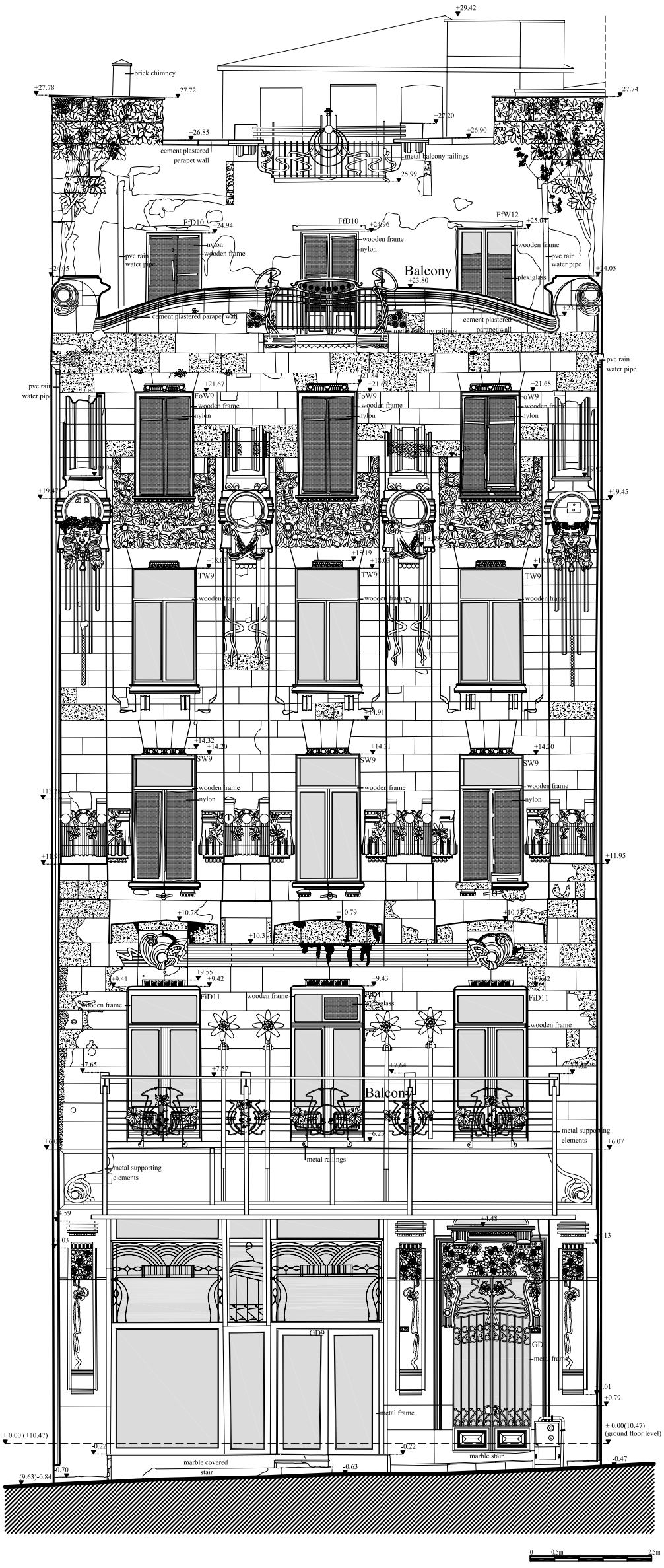

SURVEY STUDY

NORTHWEST FAÇADE

SUPERVISOR : Prof. Dr. Hasan BÖKE

DRAWED BY : Birsen PARLAK (Architect)

Figure 4. Measured façade drawing of the Botter Apartment

All architectural elements of the building were especially designed by D'Aronco (Batur 1993). Elliptical planed stairs, ornamented balustrades, stained glass windows, main and atelier ornamented entrance doors (Figure 5), the lighting elements and original elevator (Figure 6) make this building an important art object that projects the style of its period.

Figure 5. Florally ornamented main entrance door of Botter Apartment

Figure 6. Original elevator of Botter Apartment

Façade order of the apartment reflects the differentiation of residence and workplace successfully (Batur 1993). At the ground floor an asymmetrical order is seen on the façade because the main entrance of apartment is at the right side of the building. The entrance doors of the store and the apartment were decorated with flowery ornamentations. At the first floor an elliptical planed balcony is seen along the façade. The balcony has flowery ornamented railings and enlightening element.

Original façade design of D'Aronco has not changed until today except for the ground floor atelier part (Batur 1993). Ornamented atelier entrance door (Figure 7) was changed during the previous interventions. On the façade order the workplace section breaks up with five horizontal bands that have curvilinear ornaments at the edges. The upper floors that were used as a residence are in symmetrical order and also like frame

with ornamentations (Figure 8). Differentiations on the ornamentations are observed at each floor. At the fourth floor dense floral ornamentations and at the two sides of the façade under the circular medallion head of Meduza take attention with its wavy hair and crown. At fifth floor, which was designed as a setback storey, balcony emphasizes with its curvilinear ornamented railings and straight bands at two sides which have circular curves at the edges (Figure 9).

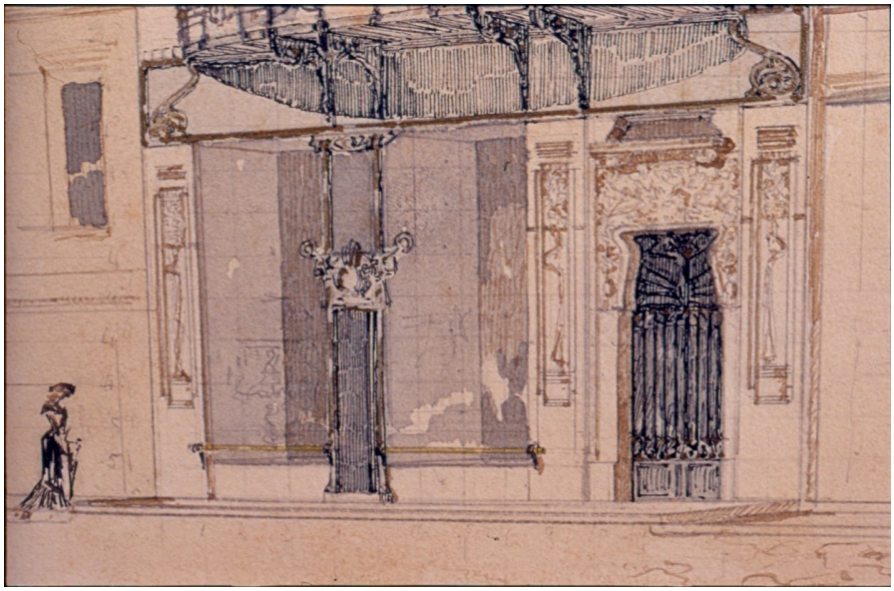

Figure 7. Original watercolor painting of D'Aronco showing the atelier and main entrance door (Source: Afife Batur Dia Archieve, Udine Civic Museum of History and Art, Udine-Italy)

Figure 8. Original watercolor paintings of D'Aronco showing the terrace and fifth floor façade ornamentations (Source: Afife Batur Dia Archieve, Udine Civic Museum of History and Art, Udine-Italy)

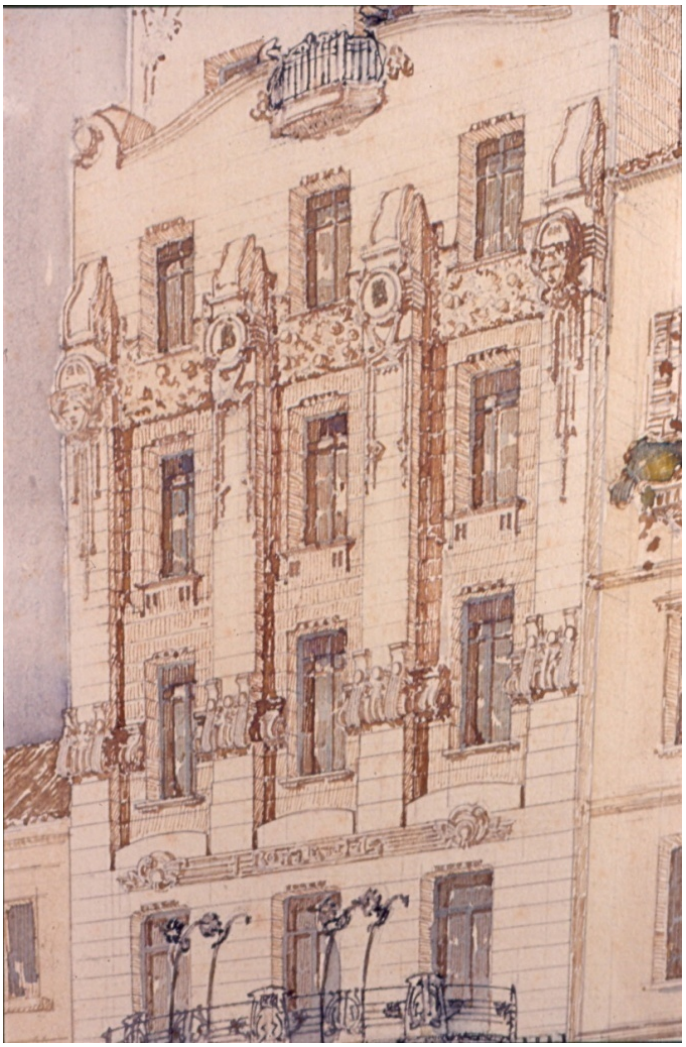

Figure 9. Original watercolor paintings of D'Aronco (Source: Afife Batur Dia Archieve, Udine Civic Museum of History and Art, Udine-Italy)

At the terrace floor the centre of the parapet wall is decorated with iron railings. The chimneys at the two sides were also decorated with dense florally ornamentations. Details of the chimney above the ornamentations cannot be.reached today. This detail is documented with a photograph taken in 1980s (Figure 10). Deterioration on the façade can be easily observed with comparing the two photographs taken thirty years apart (Figure 11).

Figure 10. Detail from the terrace floor of the Apartment at 1980s
(Source: Afife Batur archieve, photograph taken by Erkin Emiroğlu)

Figure 11. Detail from the terrace floor of the Apartment at 2009

1.2. Stones Used in the Construction of Façade of Botter Apartment

In the construction of the Botter Apartment advanced techniques were used considering the era that it was constructed. Art nouveau movement brought new construction techniques such as the use of cast iron and glass. Botter apartment was constructed in masonry system with stone and brick. Inner walls were lathing with wooden construction and brick filled. On the façade brick masonry walls were covered with ornamented limestone.

Limestone is a sedimentary rock which mainly consists of calcite crystals (Gauri and Bandyopadhyay 1999). It is formed by chemically with accumulation of shelves of tropical sea, skeleton of plants and animals and marine sediments from water solution (Schaffer 1972).

There are several types of limestone. They are shelly, crinoidal, corals and forominifera. They are substantially composed of calcite minerals and small amount of quartz. Limestone has been mostly used stones in the construction of buildings from ancient time up to the present time due to their hardness and mechanical properties (Bityukova 2006). The durability of the limestone changes according to the regions and their atmospheric conditions. One of the most important weathering processes is air pollution that rapidly deteriorates the limestone by converting it into gypsum (Diana, et al. 2007).

1.3. Air Pollution and Climatic Conditions in İstanbul

Air pollution can be defined as any atmospheric condition in which substances are higher than their normal levels (Fassina 1988). Pollutants are mixture of solid particles, liquid droplets and gases (Fassina 1988). The main sources of the pollutants are power stations, fuels for heating or industry, transportations and industrial processes.

Air pollutants are divided into two classes as primary pollutants and secondary pollutants. Primary pollutants are emitted directly from identifiable pollutant sources. These are sulphur dioxide, carbon dioxide and nitrogen oxides. Secondary pollutants are produced with the reaction of the two or more primary pollutants or normal atmospheric constituents. Secondary pollutants are sulphuric acid, nitric acid, etc.

Sulphure gases, one of the primary pollutants, are found in the atmosphere in the form of sulphure dioxide (SO_2), hydrogen sulphur (H_2S) and sulphate aerosols.

Nitrogen gases, another primary pollutant, are found in the atmosphere in the form of nitric oxide (NO) and nitrogen oxide (NO_2). Nitrogen gases are produced in high combustion temperature and other industrial operations by the combination of atmospheric oxygen and nitrogen.

Carbon oxides are found in the atmosphere in the form of carbon dioxide (CO_2) and carbon monoxide (CO). They are produced by burning oil gases, coals and forest fires.

Particulate matters and aerosols are the significant pollutants which are found in the atmosphere in form of liquid or solid substances. Aerosols are the mixtures of the fine particles with air (Fassina 1988). Particulate matters are divided into two classes; dust fall and suspended particulate matters. Dust fall is bigger in size than suspended particulate matters and suspended particles are carried out with air currents (Fassina 1988).

In this study, the effects of air pollution mainly SO_2 on limestone have been investigated in Istanbul. SO_2 levels and particulate matters (PM) concentrations in Beşiktaş - İstanbul between the years 2004 – 2009 are given in Table 1 and Table 2. A decrease is observed in SO_2 concentrations in the recent years. The highest concentrations of SO_2 are observed between October and April and it decreases in the summer months (Figure 12). This result can be explained by the consumption of more fuel for heating in winter months. Table 2 shows the particulate matters concentrations in Beşiktaş – İstanbul. Similar to the SO_2 concentration PM concentrations also reach its highest level in winter months (Figure 13).

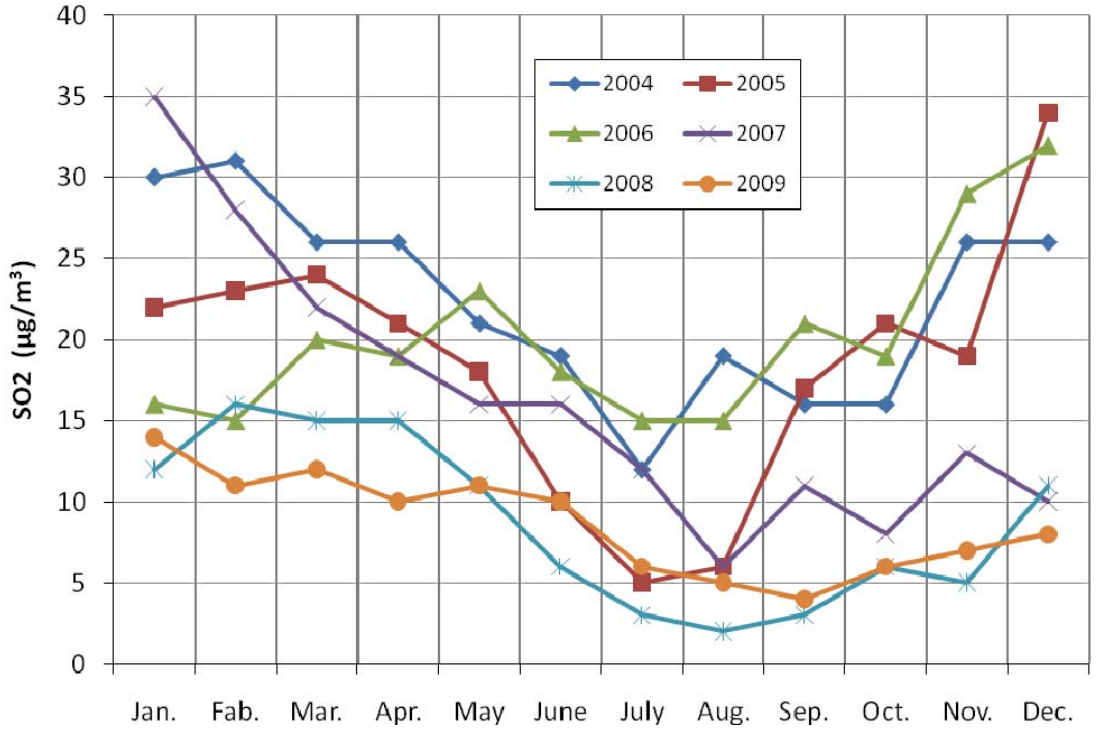

Figure 12.Monthly SO_2 concentrations in Beşiktaş - Istanbul between the years 2004 – 2009 (Source: Air Pollution Forecasting Service 2010)

Table 1. Monthly SO_2 concentrations in Beşiktaş - Istanbul between the years 2004 – 2009 (Source: Air Pollution Forecasting Service 2010)

SO_2	2004	2005	2006	2007	2008	2009
Jan.	30	39	148	92	62	67
Feb.	53	32	119	34		111
Mar.	39	37	69	18	147	111
Apr.	40	28	64	27	98	72
May	39	38	64	23	85	103
June	30	99	65	15	73	117
July	24	86	69	6	65	108
Aug.	39	59	60	15	65	100
Sep.	60	35	67	46	68	61
Oct.	82	22	40	40	62	56
Nov.	41	58	41	55	60	76
Dec.	23	31	59	90	69	73

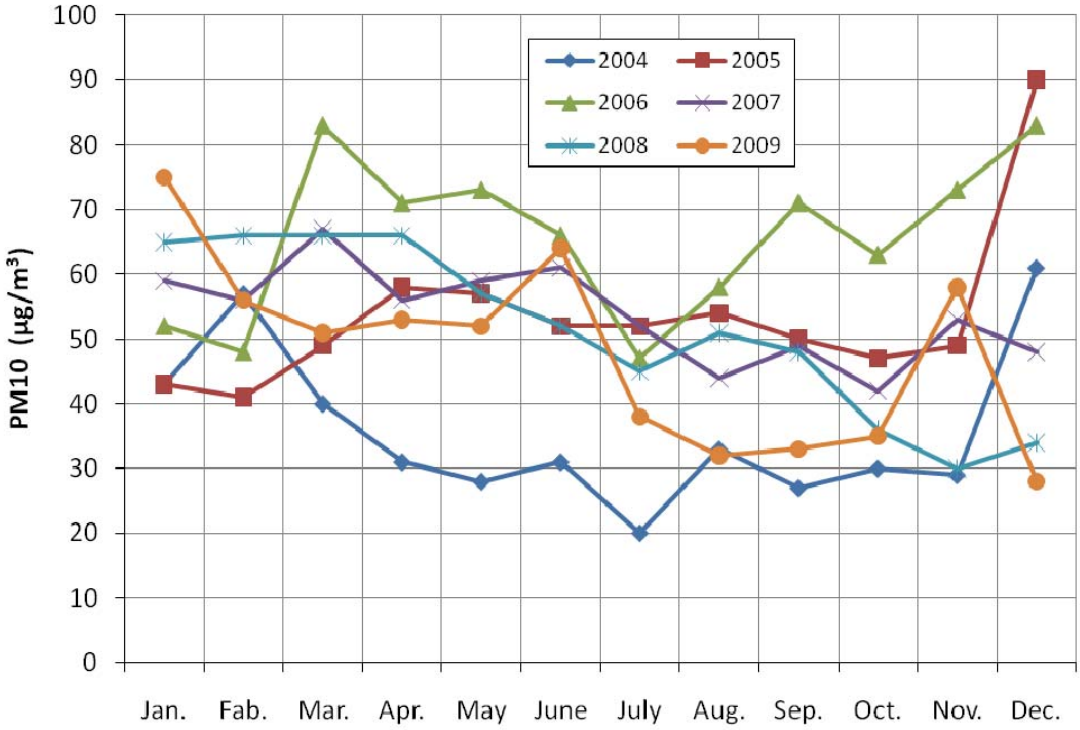

Figure 13.Monthly concentrations of Particulate Matters less than 10 µm in Beşiktaş - Istanbul between the years 2004 – 2009 (Source: Air Pollution Forecasting Service 2010)

Table 2. Monthly concentrations of Particulate Matters less than 10 µm in Beşiktaş - Istanbul between the years 2004 – 2009 (Source: Air Pollution Forecasting Service 2010)

PM10	2004	2005	2006	2007	2008	2009
Jan.	43	43	52	59	65	75
Feb.	57	41	48	56	66	56
Mar.	40	49	83	67	66	51
Apr.	31	58	71	56	66	53
May	28	57	73	59	57	52
June	31	52	66	61	52	64
July	20	52	47	52	45	38
Aug.	33	54	58	44	51	32
Sep.	27	50	71	49	48	33
Oct.	30	47	63	42	36	35
Nov.	29	49	73	53	30	58
Dec.	61	90	83	48	34	28

The impacts of air pollution show differentiations according to the climatic conditions of the regions (Bityukova 2006). The climatic condition of Istanbul is temperate and dominant wind direction is northeast but this condition changes according to seasons in the year (Çevresel Etki Değerlendirmesi ve Planlama Genel Müdürlüğü 2010).

Istanbul is located in a transition zone and has a temperate climate. The humidity is constantly high all year. The average of the annual relative humidity is between 75 – 80 % (Figure 14). Summers are hot and the average temperature is 25 ^{0}C between the July and August. Winters are cold and snowy. The average temperature is 5 ^{0}C in winter. Spring and autumn seasons are usually moderate but they also show difference from chilly to warm. The average temperature in spring and autumn is about 13 ^{0}C.

Average monthly precipitation is presented in Figure 15. Driest period is between May and July but also irregular rain fall occurs during that season. Average annual precipitation between the years 2004 – 2009 is nearly 880 mm. The wind plays important role in carrying pollutants and their concentration. Monthly average values of wind values of Istanbul are given in Figure 16. Istanbul is quite windy in all months of the year.

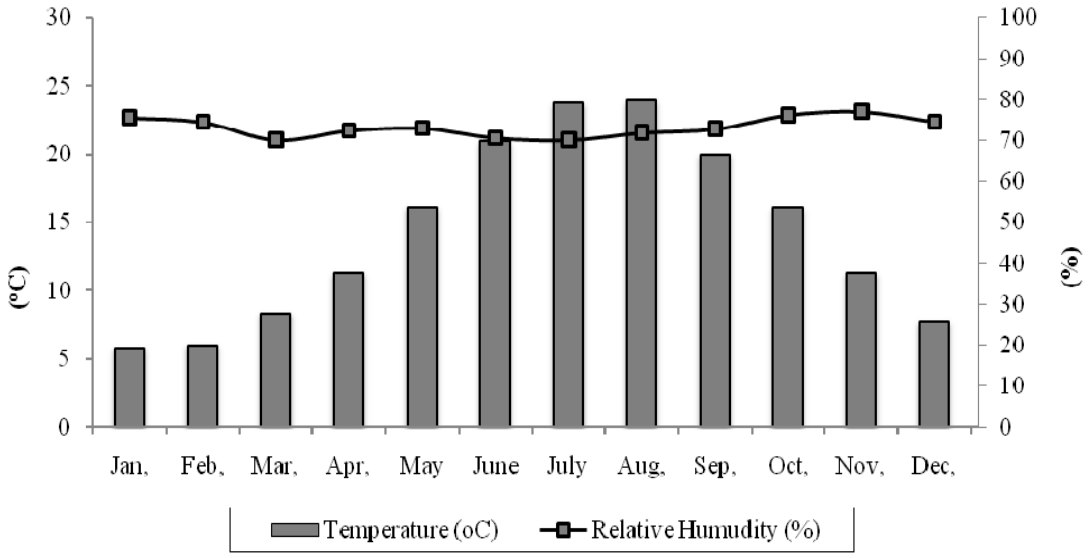

Figure 14.Monthly average values of temperature and relative humidity between the years 2000 and 2009. (Source: General Directorate of State Meteorological Affairs Ankara)

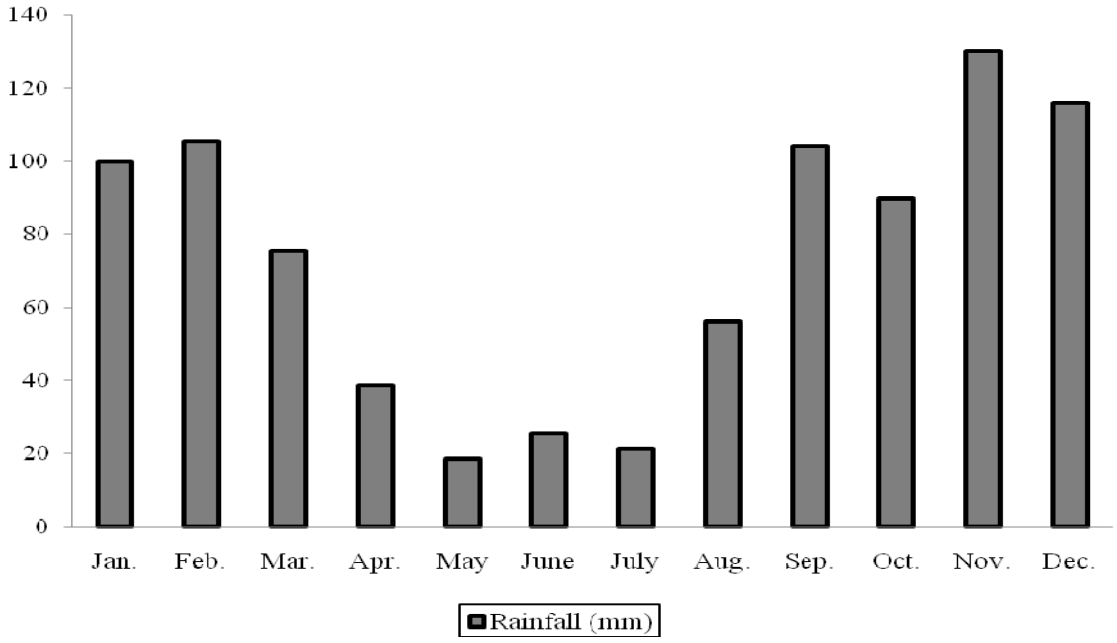

Figure 15.Monthly average values of rainfall between the years 2000 and 2009. (Source: General Directorate of State Meteorological Affairs Ankara)

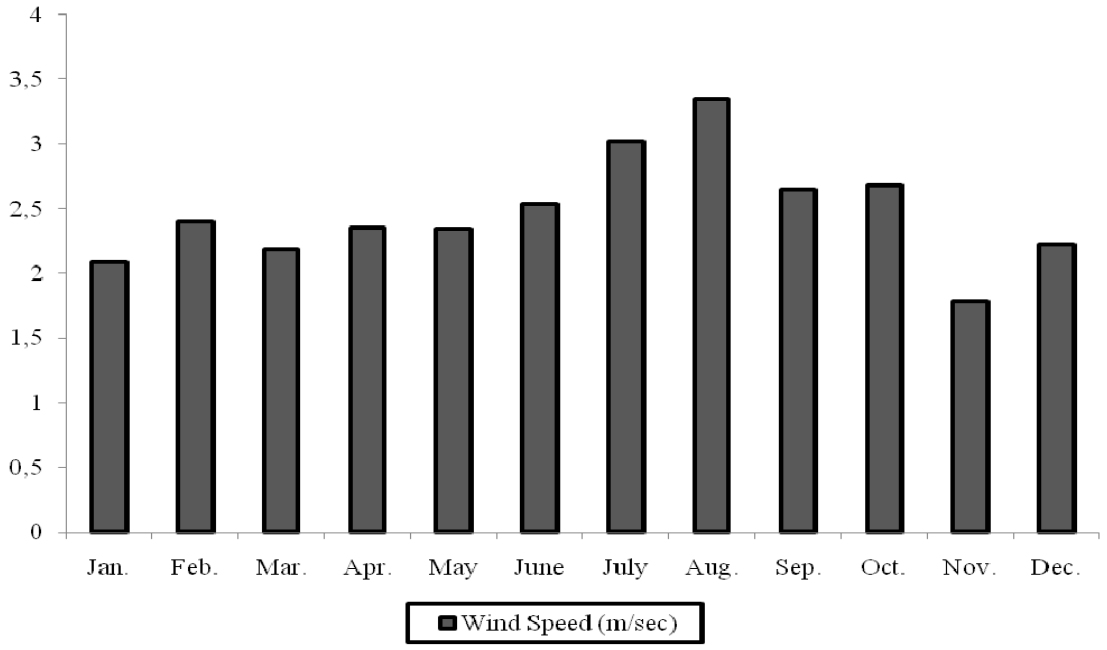

Figure 16.Monthly average values of wind speed between the years 2000 and 2009. (Source: General Directorate of State Meteorological Affairs Ankara)

1.4. Effects of Air Pollution on Limestone

Decay rates of the calcareous stones accelerated due to the use of high amount of fossil fuels since the mid 18^{th} century when industrialization began (Gauri and Bandyopadhyay 1999). Besides the natural factors such as temperature changes, precipitation, filling of the cracks by dust particles and freezing of water in the small fissures, the most affective threat on deterioration of the monuments is air pollution (Bityukova 2006).

Carbon dioxide (CO_2), sulphure dioxide (SO_2) and nitrogen dioxide (NO_2) are most effective gases in weathering process of the calcareous stones. Carbon dioxide, sulphure dioxide and nitrogen oxides do not react with carbonate minerals in calcareous stones in gas phase but they dissolve in water and react with calcite minerals (Gauri and Bandyopadhyay 1999).

The deposition of the atmospheric gases, aerosols and suspended particulate matters on the stone surface take place in two different ways; dry deposition and wet deposition.

The accumulation of the airborne pollutants such as tiny liquid droplets and tiny solid particles suspended in the air on the stone surface with the winds and turbulence is defined as dry deposition (Figure 17) (Gauri and Bandyopadhyay 1999). The transportation of the pollutants depends on the size of particles. Particles can be classified as sub-micron particles that are less than 0.1 μm, intermediate sizes from 0.5 to 10 μm and the particles larger than the 20 μm (Fassina 1988). Particles larger than the 20 μm are deposited with the gravitational settling when the air is not in motion or inertial impact (Fassina 1988). The intermediate size particles are deposited on the stone surfaces by diffusion process (Charola and Ware 2002).

Carbonate rocks react with SO_2, NO_2 and acid aerosols producing a crust largely made of gypsum ($CaSO_4.2H_2O$) (Gauri and Bandyopadhyay 1999, Diana et al. 2007). The formed crusts are mostly black or brown in color due to the embedded particles such as soot, dust and metallic particles (Gauri and Bandyopadhyay 1999). The crust formations detach from the stone surface over time. The chemical reaction of the gypsum formation with dry deposition can be expressed with following equations (1.1 and 1.2);

$$CaCO_3 + SO_2 + \tfrac{1}{2}H_2O \rightarrow CaSO_3.1/2H_2O + CO_2 \qquad (1.1)$$

$$CaSO_3.1/2H_2O + ½O_2 + 1½H_2O \rightarrow CaSO_4.2H_2O \quad (1.2)$$

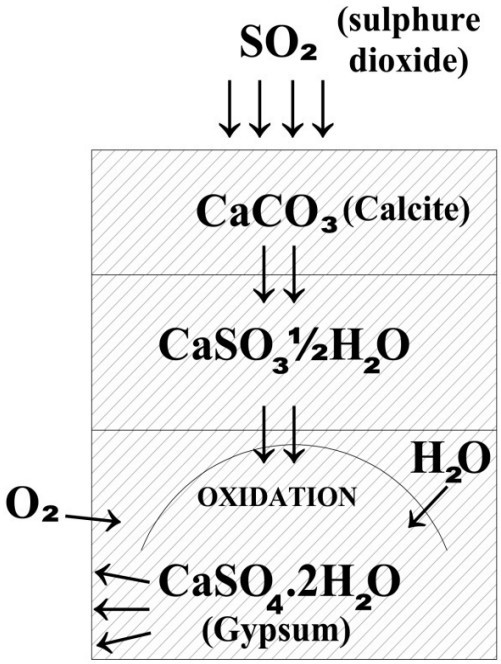

Figure 17. Gypsum formation on the stone surface by dry deposition of SO_2 (Source: Fassina 1988)

Wet deposition comprises the incorporation of trace substances in cloud droplets (rainout) and removal by falling precipitation (washout) (Fassina 1988). The efficiency of wet deposition depends on the intensity of the precipitation, the size of the rain drop, the pH value of the drops and the vertical distribution of the trace substances in the atmosphere (Fassina 1988). The pH value of the drops chances according to the air pollution concentrations. Acidity value of the rain drops increase with the SO_2 concentrations and acidic drops corrodes the calcareous stones faster in comparison to clean rain water. Rain waters dissolve the gypsum and cause the erosion of the stone surfaces.

The oxidation of SO_2 by wet deposition can be defined with two different reactions; oxidation of the sulphure dioxide in the atmosphere and on the stone surface (Figure 18). Oxidation of the sulphure dioxide in the atmosphere forms in two phases. First, sulphure dioxide dissolves in water droplets with rapid process and second phase is the oxidation of sulphure dioxide to H_2SO_4 that has a slow rate (Fassina 1988). When

the sulphuric acid (H_2SO_4) deposited on the stone surfaces reacts with calcium carbonate ($CaCO_3$) and converts it into gypsum ($CaSO_4.2H_2O$) (1.3 and 1.4).

$$SO_2 \rightarrow SO_2.H_2O \rightarrow H_2SO_4 \quad (1.3)$$

$$H_2SO_4 + CaCO_3 + H_2O \rightarrow CaSO_4.2H_2O + CO_2 \quad (1.4)$$

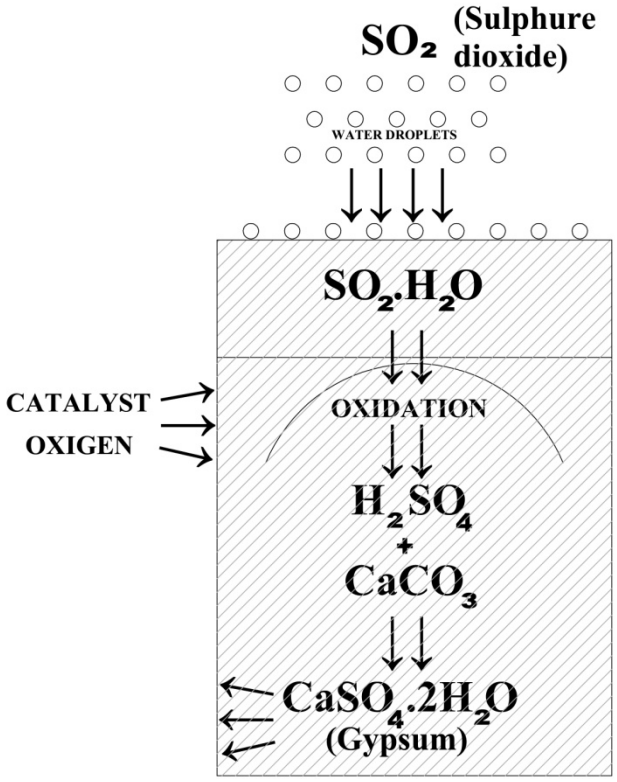

Figure 18. Gypsum formation on the stone surface by wet deposition of SO_2 (Source: Fassina 1988)

Sulphure dioxide sweeps onto the surface by condensation and then penetrates inside the stone (Fassina 1988).

Wet and dry deposition of SO_2 and condensation lead to significant deterioration on the stone surfaces. Dry deposition has a continuous and slow process compared to the wet deposition. In wet deposition, the incident precipitation washes off the previously deposited materials by dry processes and in polluted areas rainfall promotes the subsequent deposition of soluble gases (Fassina 1988).

The effects of air pollution on monuments built using calcareous stones were studied for years in the countries having high concentrations of air pollutants.

Air pollution effect on the carbonate building stones in Tallinn has been studied by Bityukova (2006). In this study, the chemical and mineralogical composition of building stone and black crust from five historical objects of Old Town of Tallinn were examined in order to reveal the weathering behavior of the limestone and estimate the influence of pollution on the decay processes. The ICP-MS analysis and X-ray diffractometer were performed. The results showed the natural origin for Ca, Mg, Si, Al, Ti, K, Na and Fe. The black crust is elevated in Cu, Pb, Sb, Sn and Zn concentrations as a result of the pollution effect. The highest increase of Cu, Pb and Zn content was determined in the samples from gypsum crust at St. Olaf's church.

The decay process of limestone in a polluted urban environment in Budapest was studied by Török (2004). In Budapest many public buildings are constructed of limestone that is susceptible to soiling and air pollution. The two most common types of stone used in Budapest. They are Miocene oolitic limestone and Pleistocene freshwater limestone (travertine). The oolitic limestone show intense crust formation and blackening. The crusts are prone to scaling and/or flaking followed by rapid substrate material loss (granular disintegration). As a consequence, significant loss in volume and decrease in strength are attributed to urban air pollution. The freshwater limestone exhibit only blackened surface crusts, but these crusts appear to be stable and they do not tend to lead to scaling.

Deterioration of limestone of building facades in Budapest have also been studied by Török (1997). On the surfaces of the building, more than 70 % gypsum has been observed. The black crusts were rich in organic matter derived from exhaust gas (soot). The decay process was explained by the crust formation, scaling and/or flaking of the crusts and rapid loss of material due to surface loss and granular disintegration.

Sulphure deposition and damage on limestone and sandstone in Stockholm city buildings have been investigated by Nord (1999). Buildings are generally covered with limestone or quartzitic sandstone. In this study, the observed damage has been expressed by digital codes. The chemical analysis was mainly undertaken with SEM/EDS. This study has verified that quartzitic sandstone is more resistant towards weathering than limestone. Coarse-grained limestone with pores and cracks are most weathering-prone. Climatic conditions and air pollution are the major causes of the degradation. In this study, significant relationships between car traffic and damage, and between car traffic and soiling, also between observed damage and present degree of sulphation at limestone surfaces were found.

Effects of air-pollution on limestone deterioration in Great Britain have been studied by Webb (1992). The sites have comprehensive air pollution. In this study, significant trend was found with limestone deterioration with increase in average sulphure dioxide concentration

Black crusts formation on travertines and factors controlling development and stability has been studied on the travertine buildings of Budapest by Török (2008). The results of the study show that extensive black crust formation is related to high concentration of atmospheric pollution and a continental climate. Black crusts contain more than 50% of acicular gypsum.

The growth of "black crusts" on the old buildings of Palermo (Sicily) was examined for the aim to distinguish between natural and anthropogenic sulphure sources. Chemical, mineralogical and isotopic composition (S-34/S-32) analyses were carried out. Sulphure isotopic compositions of gypsum-bearing crusts showed a prevailing contribution of anthropogenic sources (vehicle exhaust and other combustion processes). Natural sulphure and/or sulphate sources (biogenic and/or sea-spray) were shown to play a secondary role. These data can be considered a starting point for the determination of the rate of growth of "black crusts" in a coastal Mediterranean urban environment like Palermo (Montana, et al. 2008).

The effects of SO_2 together with ozone have been investigated in the central area of Milan. The tolerable corrosion level for limestone and copper was found higher than their normal level (Screpanti 2009).

Mapping the impact of climate change on surface recession of carbonate buildings in Europe has been done by Bonazza, et al. (2009). In this study, the Lipfert function has been taken under consideration to quantify the annual surface recession of carbonate stone, due to the effects of clean rain, acid rain and dry deposition of pollutants. The results of the study indicated chemical dissolution of carbonate stones, via the karst effect, will increase with future CO_2 concentrations, and will come to dominate over sulfur deposition and acid rain effects on monuments and buildings in both urban and rural areas.

Recession of architectural limestone in European cities was estimated after the recent reduction in sulfur dioxide in cities. The Lipfert, ICP, and MULTI-ASSESS functions were used to calculate recession from estimates of climate and air quality. It is proposed that recession rates having reached low values will remain largely unchanged over the coming century, despite likely changes in climate.

Past and future colouring patterns of historic stone buildings were predicted by Grossi (2008). The author concluded that the future offers a potential for variation in building colour, arising through different biological growth under changing climates or the presence of different pollutants. In future urban atmospheres more dominated by organic pollutants a yellowing process may be more important. Diesel soot has many organic compounds that can oxidize to brownish-coloured humic-like (HULIS) materials.

The studies on the durability of marble cladding were reviewed by Grelk (2007). In this study, the comprehensive information from more than 70 selected literature references was reviewed and discussed in order to describe the present knowledge on the causes and mechanisms responsible for the bowing and strength loss of thin marble cladding. The literature review reveals that only few researchers have examined the durability problem from a broad perspective. In addition, no conclusive answer about the mechanisms and influencing factors can be given.

Characteristics and morphology of weathering crusts on porous limestone and the role of climate and air pollution has been studied by Török. (2007). The analyses have demonstrated that the air pollution related gypsum crystallization with combination of freeze/thaw weathering lead to crust detachment with rates strongly controlled by the micro-fabric of limestone substrate.

The penetration of SO_2 into the pores of calcareous stones and the concentration of gypsum in surface layer has been estimated by Camuffo (2006). In this study, a theoretical analysis of the penetration of airborne pollutants into the porosity of calcareous stones has been made for a number of different cases. The results showed that the number of SO_2 molecules that can react with the stone decreases with increasing depth. Field observation of marble samples from monuments kept outside but sheltered from rainfall has confirmed this result. The small thickness of the sulphated layer found in both recent and archaeological stone artworks means that monuments exposed to air pollution, but sheltered from rainfall, may survive in relatively good conditions for many centuries.

Modelling of air pollution in an Italian limestone quarry by simple procedure in forecasting PM 10 dispersion was done by Degan (2006). This study aims of modelling atmospheric PM 10 concentrations in an Italian limestone quarry and the evaluation of obtained results.

The combined effect of microbial colonization by fungal growth and atmospheric pollutants in the sulfation of Scaglia limestone, which is a very common building material in ancient monuments in Central Italy, was investigated by means of laboratory experiments of dry deposition of sulfur and nitrogen dioxides. Results indicate a combined action of particulate matter deposition and sulfation in the formation of gypsum on the samples exposed outdoors, and to a significant influence of fungal growth in the conversion of metal sulfide particulate matter to sulfate thus promoting subsequent formation of gypsum also in the absence of pollution (Moroni, et al. 2004).

Microbial growth and air pollution in carbonate rock weathering was also studied by Pitzurra (2003). In this study, preliminary results on Scaglia limestone weathering caused by air pollution and microbial colonization are presented. Outdoor exposure experimental assays were performed on samples. Samples were exposed in two areas in Perugia (Italy) that differ in degree of urban air pollution. At different times of exposure, ranging from 1 to 12 months, microbial contamination of sampled surfaces was evaluated by microbiological techniques, genotyping and scanning electron microscopy. After I year of exposure, a significant fungal colonization and the presence of weathering products (i.e., gypsum) were detected.

Damage functions and equations of Massangis limestone exposed to ambient atmospheric conditions were established by Delalieux (2002). In this study, limestone slabs were placed in five different environments in Belgium and run-off water was collected for chemical analyses, over a 3 yr period. Mechanism equations and damage functions were first established for each of the five studied sites. A damage function was proposed and compared with limestone damage functions found in the literature.

In Turkey the effects of air pollution have been studied on calcareous stones used in monuments and recent buildings. In Sivas, the gypsum formation in carbonate stone by air pollutants has been investigated on samples taken from the unsheltered surfaces of 13 historical buildings of different ages. The results of the study showed that the gypsum formation on polluted surfaces has been caused and influenced by the polluted atmosphere of Sivas city, high relative humidity, the age of the buildings and stone characteristics (Fresenius Environmental Bulletin 2002).

Deterioration of limestone used in Sehzade Mehmed Mosque and other monuments due to action of air pollutants in Istanbul have been examined by Tugrul (1998). The acceleration in deterioration of building stones has been attributed to air

pollution. Deterioration of the limestone under polluted atmospheres was investigated through petrographical, chemical and mineralogical analyses. Studies have shown that action of air pollutants and changes in meteorological factors are the more effective factors than the petrographical and physical characteristics of the the rocks.
(Tuğrul and Zarif 1998, 1999)

The effects of the environmental conditions on historical monuments in Konya (Turkey) have been studied by Çınar (1999). In Konya atmosphere, a great amount of the gases NO_x, CO_2 and SO_2 are released from the chimneys of houses and factories, the exhaust of cars and trains. These gases accelerate the deterioration of the stones used in the construction of monuments and concrete buildings in Konya (Çınar, et al. 1999).

The accelerating effects of the microorganisms on biodeterioration of stone monuments under air pollution and continental-cold climatic conditions in Erzurum, Turkey have been studied by Nuhoğlu (2006). Studies have been carried out on specimens of the Rustempasa Bazaar, the Lalapasa Mosque, the Erzurum Castle Mosque, the Double Minarets-Madrasah, the Great Mosque and the Haji Mehmet Fountain aged from 441 to 823 years old. The results showed that vegetative and reproductive (generative) forms of the microorganisms and gypsum could develop especially during the winter months (Nuhoğlu, et al. 2006).

The effects of air pollution on travertines in Ankara have been studied by Böke et al (1992). In this study extensive gypsum formation has been detected in sheltered surfaces from rain whereas it has been observed in small amounts in unsheltered surfaces. This formation has been explained in relation to structure and composition of travertine, pollution and climatic parameters of Ankara and ages of the buildings (Böke, et al. 1992).

1.5. Protection of Calcareous Stones From the Air Pollution

Gypsum formations on the stone surfaces increases with moisture, high SO_2 concentrations, nitrogene oxides (NO_x) and carbon particles (Böke, et al. 1999, Cheng, et al. 1987, Gauri, et al. 1982/1983, Göktürk, et al. 1993). Basic way of preventing the deterioration of the stone is to decrease the concentration of SO_2 and protecting the stone surfaces from rain water. Besides these general precautions the studies for the protection of stone surfaces can be divided into four groups.

The first group of studies are reconversion of gypsum into the $CaCO_3$ by using carbonate solutions (Skoulikidis and Beloyannis 1984, Alessandrini, et al. 1993). When the gypsum reconverted to CaCO3, forms in powder on the stone surface and so it is not suggested.

The second groups of studies are usage of polymer materials as a surface protective agent (Alessandrini, et al. 1993, Atlas, et al. 1988, Striegel, et al. 2003, Thompson, et al. 2003, Elfving, et al. 1994, Gauri, et al. 1973, Cimitan, et al. 1994). The polymers decrease the effects of SO_2 in short term but in long term this effect disappears and deterioration increases. And also polymers lost their thermoplastic properties in time and this should send away from the stone surfaces with the unfavorable mechanic methods.

The third groups of studies are decreasing the solubility of $CaCO_3$ by using surfactants. Gypsum formation is decreased in proportion of 10% under the laboratory conditions (Böke, et al. 2002).

The fourth group of studies are getting resist calcite surface to the acidic conditions by applying anionic surfactants such as phosphate, oxalate and oleate on calcite surfaces (Böke and Gauri 2003, Thompson, et al. 2003). When these surfactants are used calcium oxalate and calcium oleate layers form on the $CaCO_3$ surface (Böke, et al. 2003). These formations on the surface decrease the effects of SO_2 on the calcareous stones approximately 15% (Böke and Gauri 2003).

In a new and interesting study, the efficiency of four different biodegradable polymers as protective coatings on marble–SO_2 reaction were investigated. The result of the study showed that the use of high molecular weight PLA (HMWPLA) polymer on marble surfaces provided significant protection up to 60% (Ocak, et al. 2009).

1.6. Aim of Study

The aim of this study is to investigate the façade of the historical Botter Apartment affected from air pollution and to document the circumstance with regard to the results of the analyses. The important task is to state the present conditions of the deterioration and also further aim of this study is to propose preservation treatments and appropriate intervention methods for restoration works of the monument.

In this study present situation of the façade was documented by photographs and drawings. Experimental studies were carried out on collected samples by laboratory works to determine the basic physical properties, mineralogical compositions, chemical compositions and microstructural properties. These studies allow establishing the deterioration process of limestone used in the historic and new buildings in the polluted environment of Istanbul.

CHAPTER 2

EXPERIMENTAL METHODS

In this study, air pollution effects on the limestone were analyzed on the façade of the Botter Apartment located in Beyoğlu – Istanbul. In order to determine the present conditions of façade, samples were collected and their basic physical, mineralogical, chemical and microstructural properties were analyzed.

2.1. Site Survey

The site survey of the study was done between the October and December 2008. First measured survey of the façade of Botter apartment was completed. Sketch of the façade was not prepared. Previous drawings of the building were used during the measurement.

The measurement of the façade was done by using total station theodolite. Photographs of every single detail were taken during the measured survey. After the measurement survey was completed, recorded readings conveyed to the computer with dwg extension. Two dimensional drawing of the façade was prepared in AutoCAD 2009 program. Weathering forms observed on the stone surfaces were then documented on the drawing of the façade with notes and photographs.

2.2. Sampling

Samples were collected from the different levels of the front façade. Samples were collected from the first floor, balcony of the fifth floor and the roof floor. From surface to approximately 5 mm inside was named as Weathered Layer-1, approximately from 5 mm to 15 mm inside was named as Weathered Layer-2 and unreacted parts was named as Unweathered Layer. (Figure 19).

Black crust formation observed samples were collected from the First and Roof Floor. Fifth Floor sample was chosen from corroded surface. Because of closed

windows sample was not taken from other floors. The collected samples are given in Table 2.1. (Figure 20).

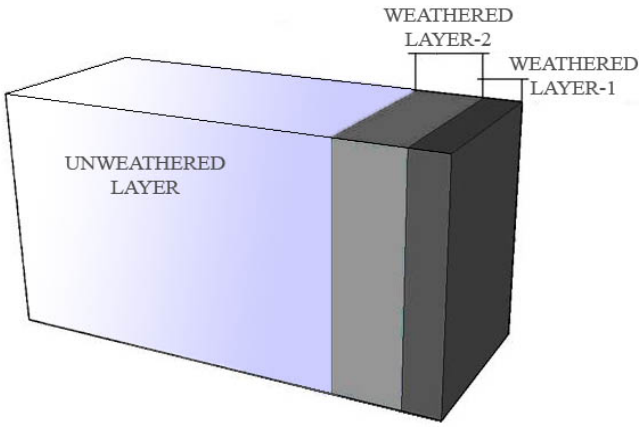

Figure 19. Schematic view of the layers

Table 3. List of samples

Sample Name	Sample Layers	Sample Definition
Roof Floor Sample (RFS) (Figure 21)	RFS-W1-Weathered Layer-1 (0-5 mm)	Stone sample from the roof floor which sheltered from the rain on the front facade
	RFS-W2- Weathered Layer-2 (5 mm-15 mm)	
	RFS-UW- Unweathered Layer	
Fifth Floor Sample (FfFS) (Figure 22)	FfFS-W1- Weathered Layer-1 (0-5 mm)	Sill Stone sample from the fifth floor which rain washed place of the front facade
	FfFS-W2- Weathered Layer-2 (5 mm-15 mm)	
	FfFS-UW- Unweathered Layer	
First Floor Sample (FsFS) (Figure 23)	FsFS-W1- Weathered Layer-1 (0-5 mm)	Stone sample from the first floor which sheltered from the rain on the front facade
	FsFS-W2- Weathered Layer-2 (5 mm-15 mm)	
	FsFS-UW- Unweathered Layer	

İZMİR INSTITUTE OF TECHNOLOGY

THE GRADUATE SCHOOL OF ENGINEERING AND SCIENCES

A MASTER THESIS ON ARCHITECTURAL RESTORATION

AIR POLLUTION EFFECTS ON THE FAÇADE OF THE BOTTER APARTMENT IN İSTANBUL

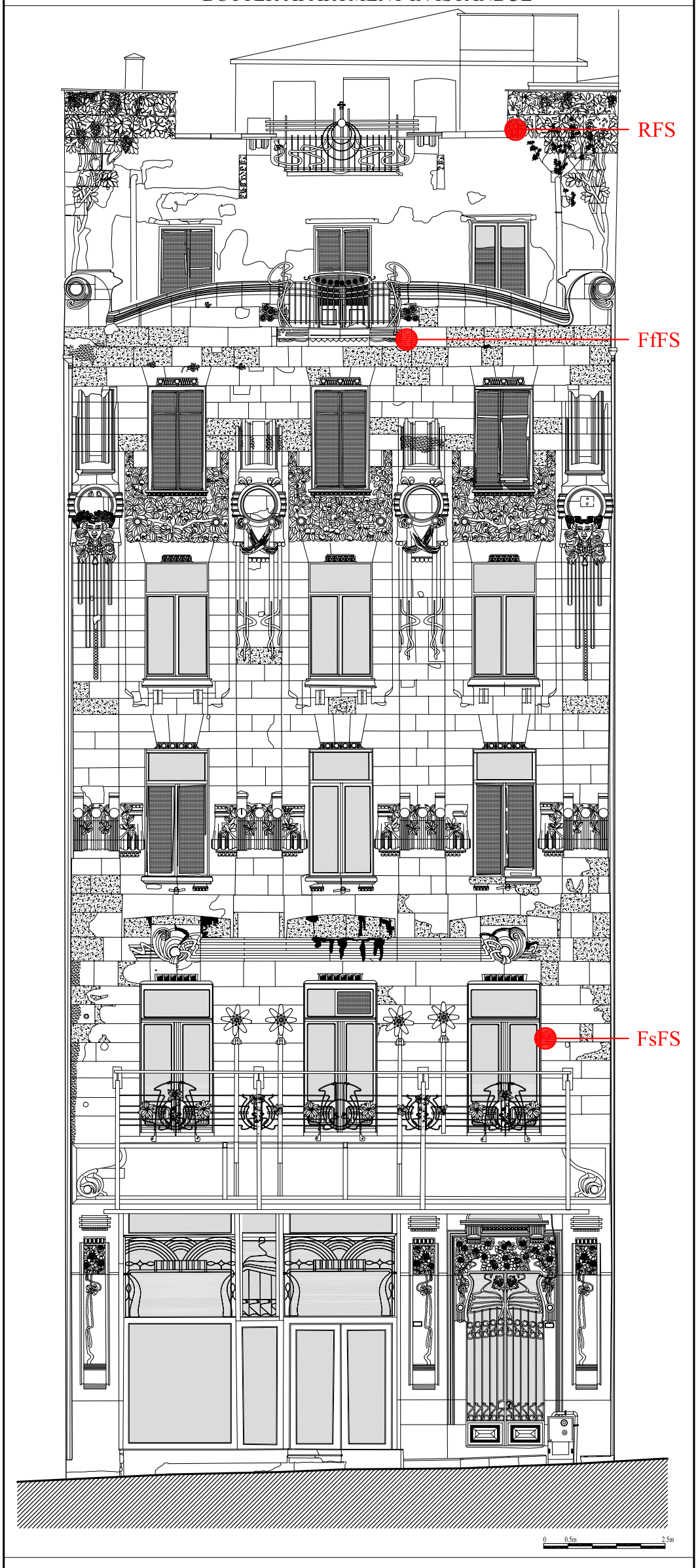

SAMPLE PLACES

NORTHWEST FAÇADE

SUPERVISOR : Prof. Dr. Hasan BÖKE

DRAWED BY : Birsen PARLAK (Architect)

Figure 20. Façade of the Botter Apartment showing the places of the samples taken from

Figure 21. Figure showing the place of Roof Floor Sample (RFS) taken from.

Figure 22. Figure showing the place of Fifth Floor Sample (FfFS) taken from.

Figure 23. Figure showing the place of First Floor Sample (FsFS) taken from.

2.3. Experimental Study

Several laboratory tests were carried out in order to determine their basic characteristics of the collected samples.

These are;

- Basic physical properties (RILEM standart and SEM-EDS).
- Mineralogical compositions (XRD and FT-IR analysis).
- Chemical compositions (SEM-EDS and FT-IR analysis).
- Micro structural properties (SEM-EDS analysis).
- Determination of weight loss (TGA analysis).

2.3.1. Determination of Basic Physical Properties of Limestone

Bulk densities and porosities of the stones were determined by using RILEM standard test methods (RILEM 1980) .A bulk density is the ratio of the mass to its bulk volume in units of grams per cubic centimeters (gr/cm^3). Porosity is the ratio of the pore volume to the bulk volume of the sample.

Density and porosity analyses were carried on two samples. The samples were dried in oven at 40 ºC at least 24 hours. Dried samples were weighed by a precision balance (AND HF-3000G). Then dried samples were immersed in distilled water in vacuum oven (Lab-Line 3608-6CE) to completely fill the pores. Saturated weights (M_{sat}) and Archimedes weights (M_{arch}) are measured with hydrostatic weighing in distilled water were measured by a precision balance.

Using the dry, saturated and hydrostatic weights, densities and porosities of the samples were calculated by the following formula (2.1 and 2.2):

$$\text{Density D (g/cm3)} = M_{dry} / (M_{sat} - M_{arch}) \quad (2.1)$$

$$\text{Porosity P (\%)} = [(M_{sat} - M_{dry}) / (M_{sat} - M_{arch})] \times 100 \quad (2.2)$$

In the formula:

M_{dry} : Dry Weight (g)

M_{sat} : Saturated Weight (g)

M_{arch} : Archimedes Weight (g)

$M_{sat} - M_{dry}$: Pore Volume

$M_{sat} - M_{arch}$: Bulk Volume

Porosities of the stones were also determined by using Philips XL 30S-FEG Scanning Electron Microscope (SEM) by phase analyses on SEM pictures. Also texture of the used limestone on the façade of the Botter apartment was analyzed by using SEM analyses.

2.3.2. Determination of Mineralogical Compositions of Limestone

Mineralogical compositions of stones were determined by X-ray Diffraction analysis performed by using a Philips X-Pert Pro X-Ray Diffractometer (XRD) and FT-IR analyses by using a Perkin Elmer FT-IR system spectrum BX spectrometer. The samples with particle size less than 53 μm were used for XRD and FT-IR analyses. For FT-IR analysis, samples were dispersed in 70 mg of KBR and pressed into pellets under about 10 tons/cm^3 pressure. Spectra were acquired in between 400 – 4000 cm^{-1}.

2.3.3. Determination of Chemical Compositions and Microstructural Properties of Limestone

Chemical compositions and microstructural properties of the stones were determined by using Philips XL 30S-FEG Model Scanning Electron Microscope (SEM). SEM-EDS analysis performed on the three layers; weathered, under weathered and unweathered layers of the stones.

2.3.4. Determination of Weight Loss of Limestone by Thermogravimetric Analysis

Both weathered layer and unweathered layers of the lime stones were analyzed by thermogravimetric analysis (TG/DTG) by using Shimadzu TGA-21 to determine % weight loss by heating. TGA analysis was carried out in static nitrogen atmosphere at a temperature range of 25 – 1000 ºC.

CHAPTER 3

RESULTS AND DISCUSSION

This chapter includes the experimental results of the limestone affected from the air pollution. Densities and porosities of the stones, mineralogical and chemical compositions and microstructural properties are explained and discussed.

3.1. Visual Analysis of Weathering Forms Observed on the Façade of the Botter Apartment

Historic Botter Apartment has not been used for years and lost its function. Furthermore the modifications needed for the different new functions cause loses of many original materials. The entrance of the workshop totally lost its original design in 1962 for conversion into the branch of a bank (Batur 1993). The materials used on the façade of the apartment were also damaged due to the air pollution and lack of maintenance.

The metal elements were corroded and changed their original colors. In addition to this, metal supporting elements of the balcony were further oxidized and the balcony is now under demolition threat.

Most of the window frames and glass were broken and they are covered with nylon. The most serious damage is seen on the roof. Some parts of the roof are collapsed and now it is exposed to rain water.

The main weathering forms observed on the stone surface were considered in three headings and showed with mapping (Figure 24). First, the loss of stone material in the form of break out (Figure 25) and back weathering due to the loss of black crust (Figure 26), the second discoloration and deposit in the form of coloration (Figure 27), microbiological colonization (Figure 28), black crust (Figure 29) and higher plants (Figure 30) and third, detachment in the form of scaling (Figure 31). The listed weathering forms material deteriorations showed on the drawing of the Botter Apartment façade (Figure 32).

İZMİR INSTITUTE OF TECHNOLOGY

THE GRADUATE SCHOOL OF ENGINEERING AND SCIENCES

A MASTER THESIS ON ARCHITECTURAL RESTORATION

AIR POLLUTION EFFECTS ON THE FAÇADE OF THE BOTTER APARTMENT IN İSTANBUL

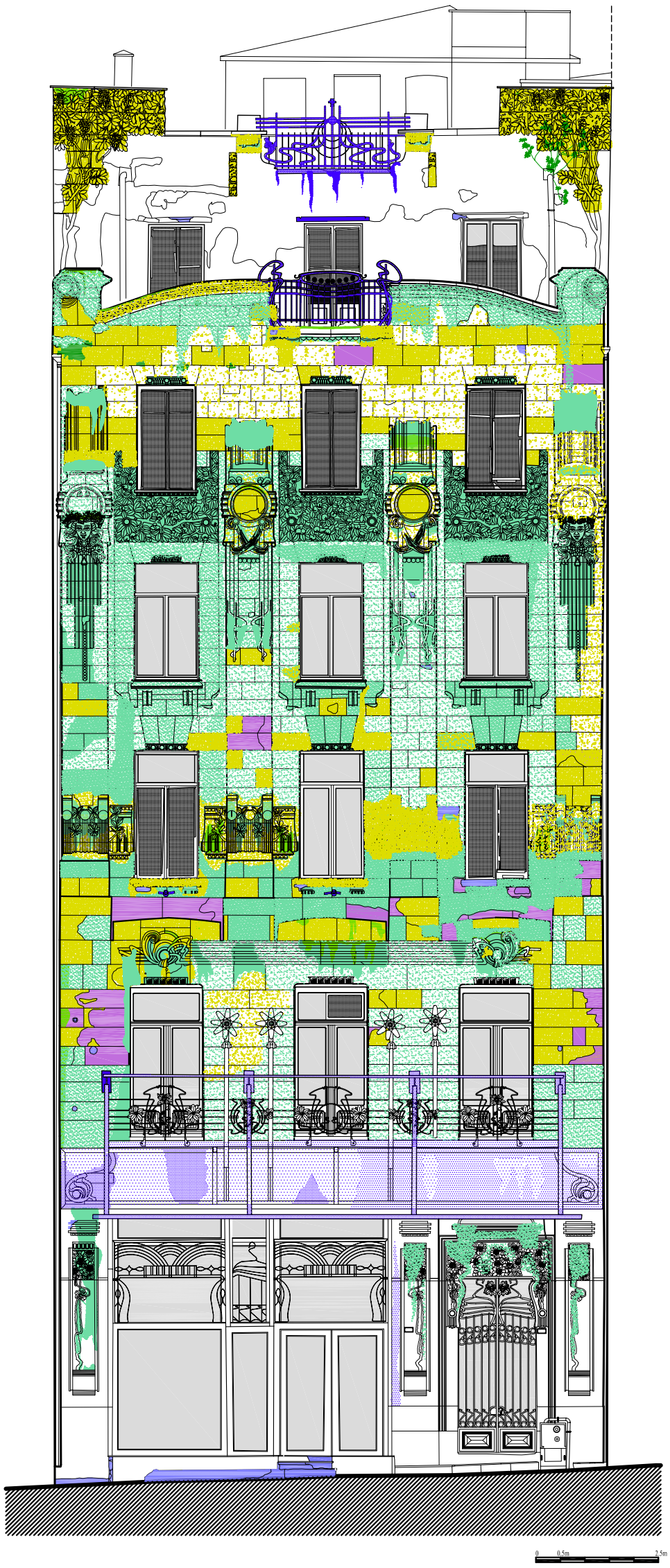

VISUAL ANALYSIS

NORTHWEST FAÇADE

SUPERVISOR : Prof. Dr. Hasan BÖKE

DRAWED BY : Birsen PARLAK (Architect)

WEATHERING FORMS

- Black Crusts
- Grey Crusts
- Back Weathering due to the loss of Black Crusts
- Scaling
- Microbiological Colonization
- Break Out
- Higher Plants
- Coloration

Figure 24. Mapping of weathering forms observed on the façade of the Botter Apartment

The weathering forms occur for many reasons. First, loss of stone material in the form of back weathering on the stone surfaces occurs with the effect of the black crust. Black crust is a gypsum formation and easily dissolves with the rain water so that uniform loss of stone material was seen parallel to the stone surfaces. The loss of stone material in the form of break out occurs due to the constructional causes. Break out of stone fragments mostly observed on the ornaments and sills, these are mostly effected parts from the black crust.

In the head of discoloration and deposits four weathering forms were observed. Coloration is the changing of the original stone color due to the chemical weathering of the minerals (Fitzner and Heinrichs 2001). Black crust was mostly observed weathering form on the stone surfaces. Crusts which are grey to black colored deposits on the stone surfaces and changes in the morphology of the stone surfaces (Fitzner and Heinrichs 2001). Microbiological colonization and higher plants are both biological colonizations. The main reason of the biological colonizations is the dampness.

The detachment on the stone is observed in the form of scaling. Scaling is the detachment of the stone pieces parallel to the stone surfaces but is not followed by any stone structure (Fitzner and Heinrichs 2001). Scaling that observed on the Botter apartment is detachment of the black crusts.

Figure 25. Break out on the façade of the Botter Apartment

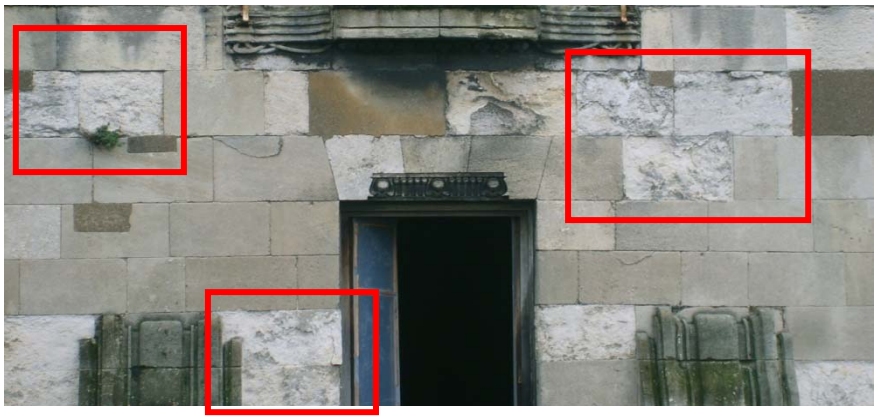

Figure 26. Back weeathering due to the loss of black crust

Figure 27. Coloration due to the corrosion products of the metals

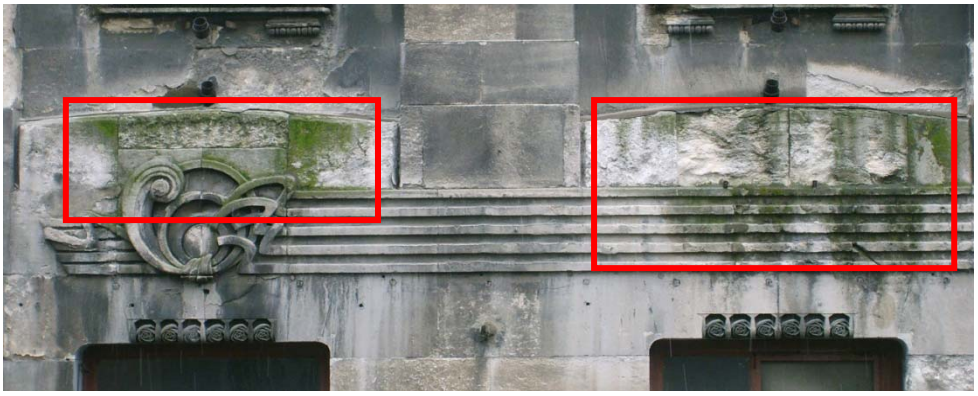

Figure 28. Microbiological Colonization on the façade of the Botter Apartment

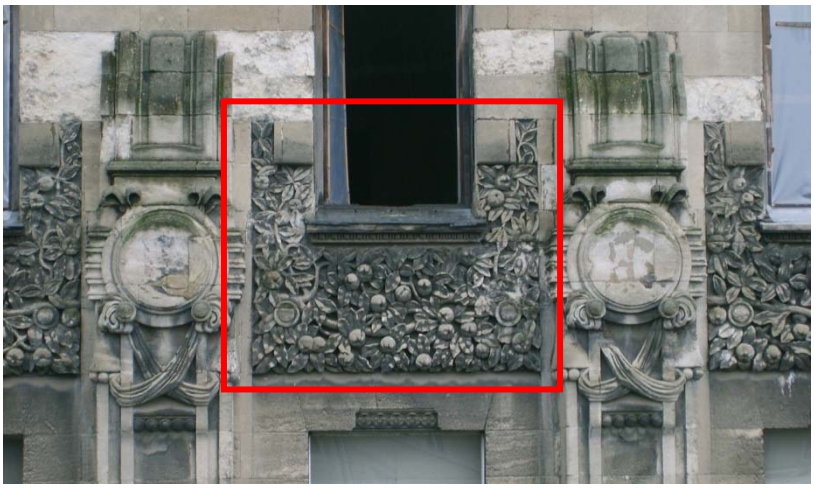

(a)

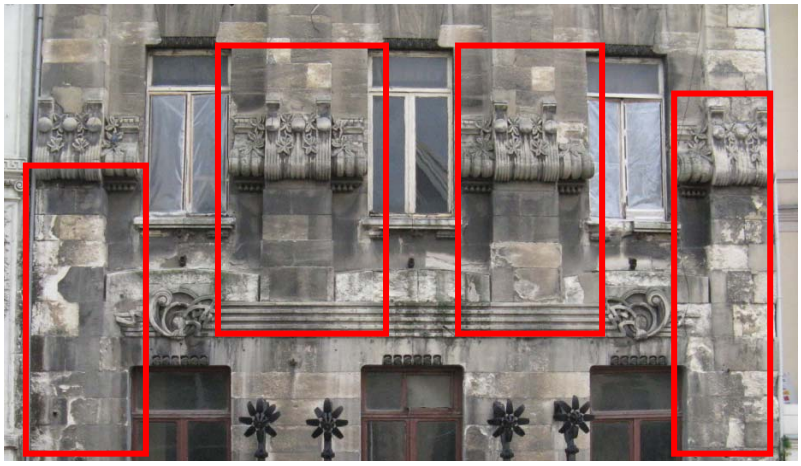

(b)

Figure 29. Black Crust on the façade of the Botter Apartment

Figure 30. Higher Plants on the façade of the Botter Apartment

Figure 31. Scaling on the façade of the Botter Apartment

Figure 32. Present condition of the Botter Apartment

3.2. Basic Properties of Limestone

Limestone used on the façade of the Botter Apartment is mainly composed of calcite minerals of sea shell and corals (Figure 33). The texture of the limestone used on the façade of the Botter Apartment was analyzed by SEM analyses. SEM analysis indicated that limestone used on the façade of the Botter Apartment is mainly composed of calcite minerals of sea shell and corals (Tuğrul and Zarif 1998).

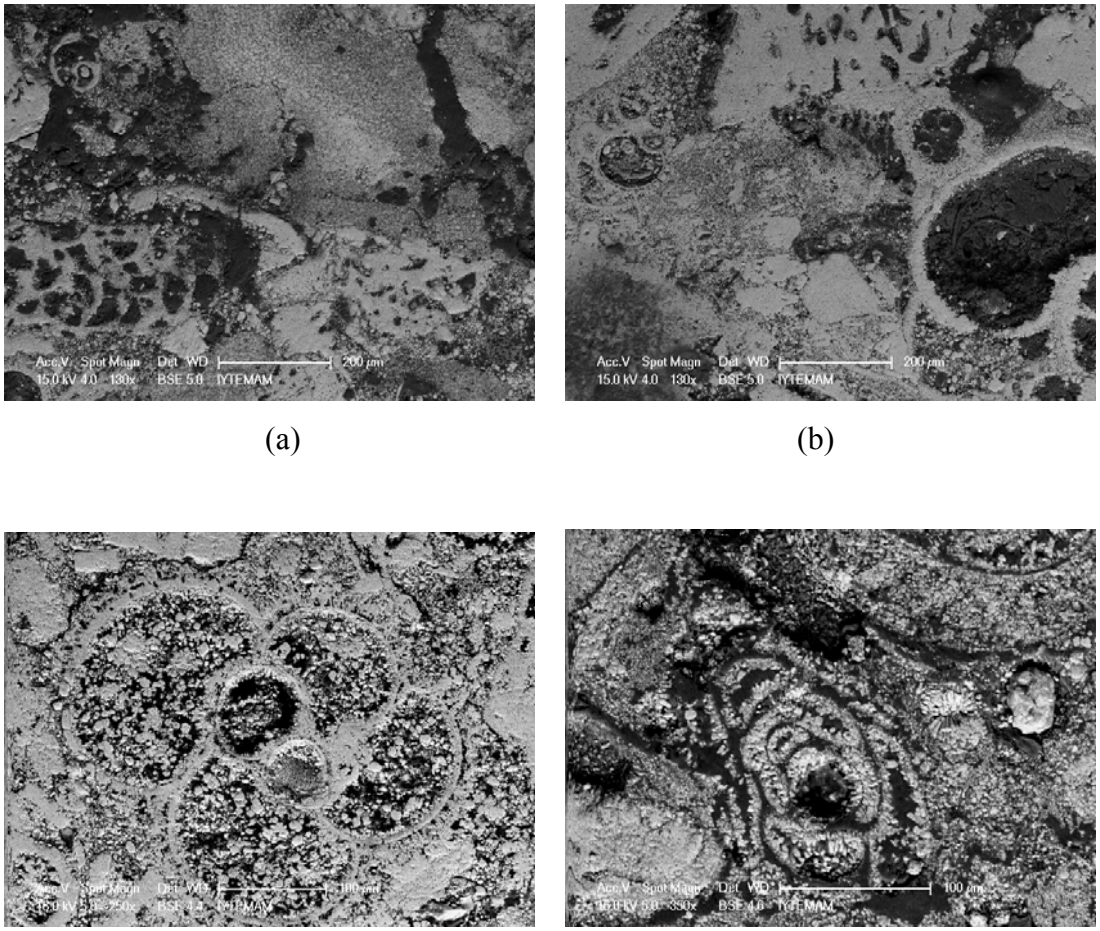

(a) (b)

(c) (d)

Figure 33. SEM images of limestone showing calcite minerals, the sea shell and corals in composition with a magnification setting of (a) and (b) 130 x, (c) 250 x and (d) 350 x and accelerating voltage 15 kV

Bulk density and porosity values of the unweathered parts of the limestone were determined using RILEM standard test methods. Density and porosity values of the limestone are about 2.08 g/cm^3 and 23.44 % by volume respectively. Change of porosity values from surface to inside were determined by SEM-EDS analysis.

Samples taken from the first floor and roof floor were examined with SEM analyses from the surface to the inner parts to see the differences in porosity values. Results of the SEM analyses show that porosity of the limestone increased through the weathered surface. Porosity values of the first floor and the roof floor samples were measured until the sulphure values of the samples reach the zero value.

At the first floor sample (FsFS) decrease of porosity was observed through inside of the stone (Figure 34). Roof floor sample (RFS) was analyzed approximately 8 mm inside of the stone (Figure 35). High porosity values were observed near the surface of the stone.

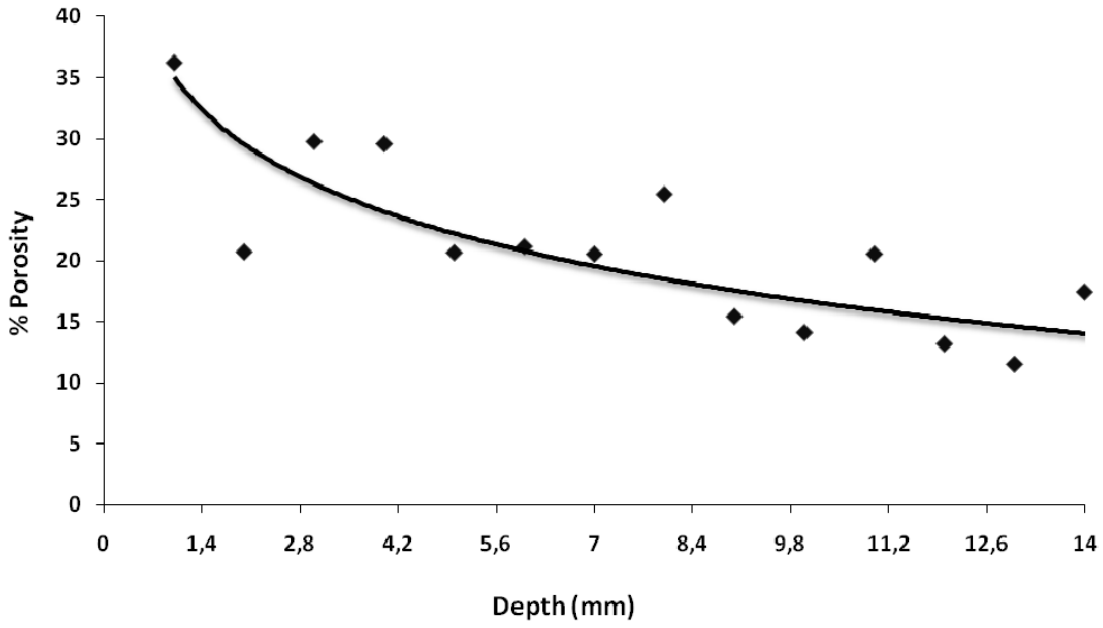

Figure 34. Porosity values of the FsFS from surface to the inner.

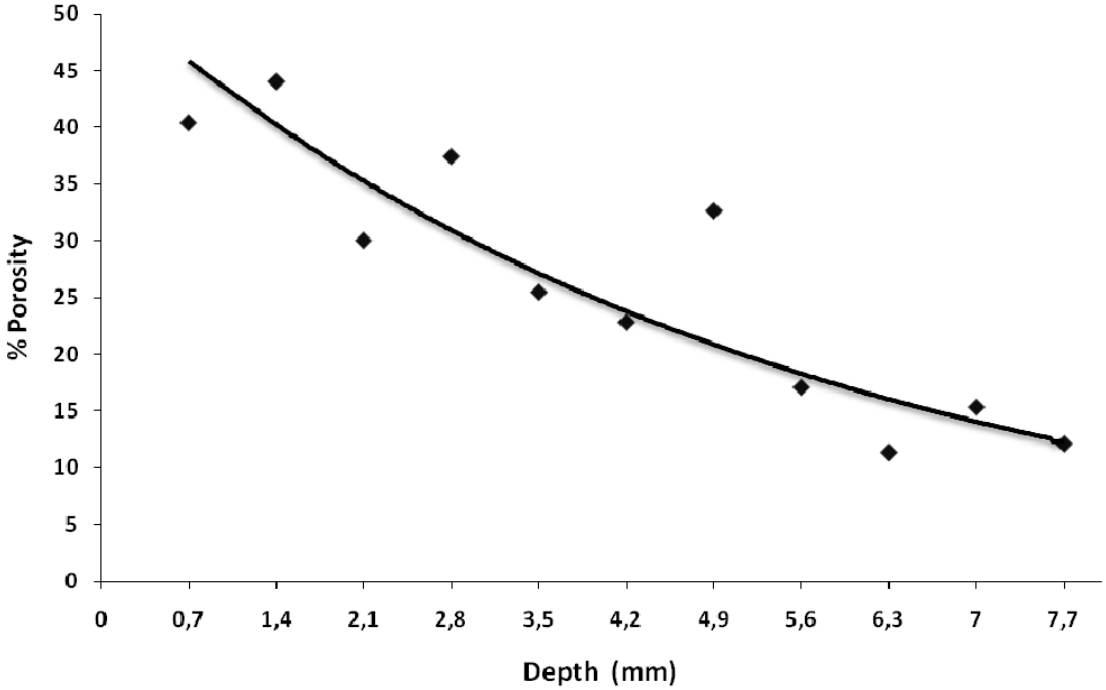

Figure 35. Porosity values of the RFS from surface to the inner

Air pollution changes the mineralogical properties of the stone and this leads to change in physical properties. The effect of porosity on damage was mentioned in the study of Lefévre and Ausset (2002). When the stones have high porosity rain rapidly penetrates to the inner parts before running off the surface. After this situation, during the drying phase, water evaporating leads to the crystallization of dissolved salts which are mainly gypsum ($CaSO_4.2H_2O$) in the polluted environments. Below the stone surface its formation facilitates the detachment of the stone slabs. When the slab detached from the surface it leaves an open new surface being subjected to the air pollution.

3.3. Mineralogical Compositions of Limestone Samples

3.3.1. Mineralogical Compositions of Unweathered Limestone

Mineralogical compositions of the limestone collected from façade of the Botter Apartment were determined by XRD and FT-IR analysis. X-ray diffraction (XRD)

analysis of the unweathered parts of the samples indicated that they were mainly composed of calcite minerals (Figure 36).

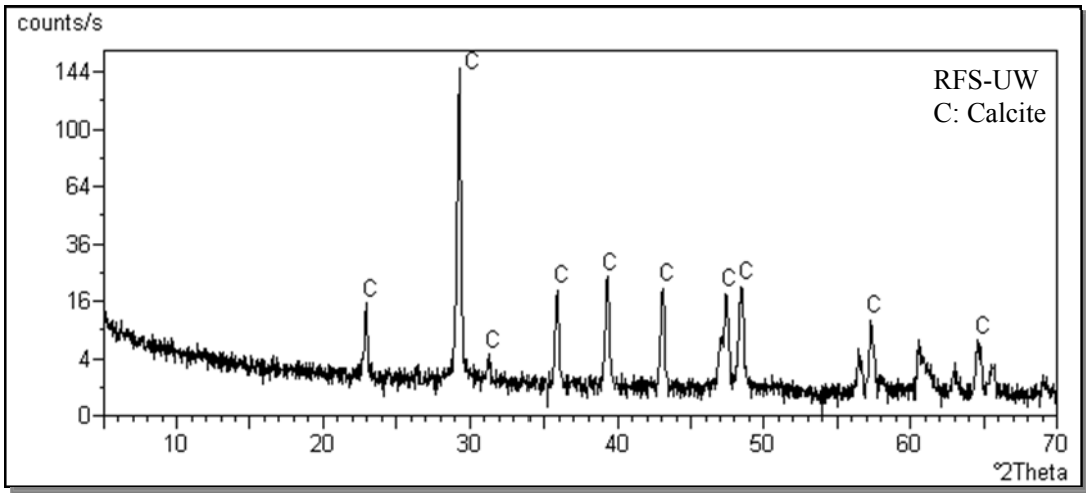

(a)

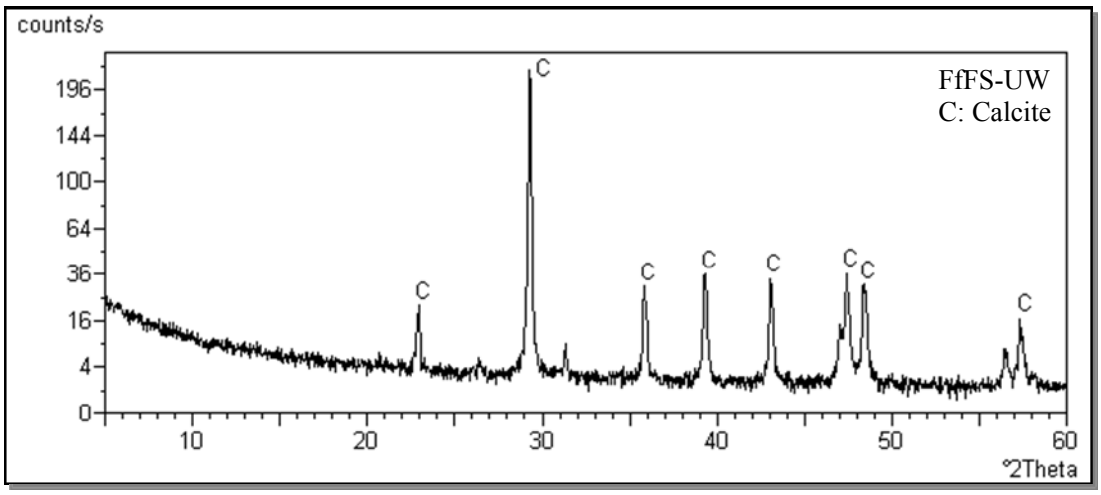

(b)

Figure 36. XRD patterns of the Unweathered Layer of the samples (a): Roof Floor Sample (RFS-UW), (b): Fifth Floor Sample (FfFS-UW), (c): First Floor Sample (FsFS-UW)

(Continued on next page)

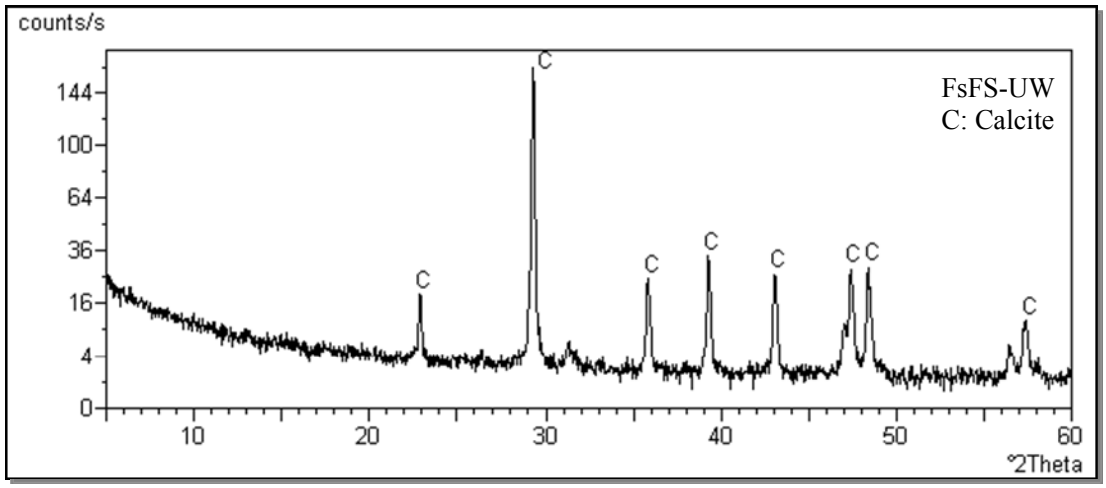

(c)

Figure 36. (Cont.)

Mineralogical compositions of the unweathered parts of the collected samples were also determined with FT-IR spectrum. The unweathered parts of the samples were taken from the 15-30 mm inside from the surfaces of limestone. In the FT-IR spectrum of the unweathered limestone the strong absorption bands of Carbonate at 1453 cm^{-1} and 873 cm^{-1} were indicated (Figure 37).

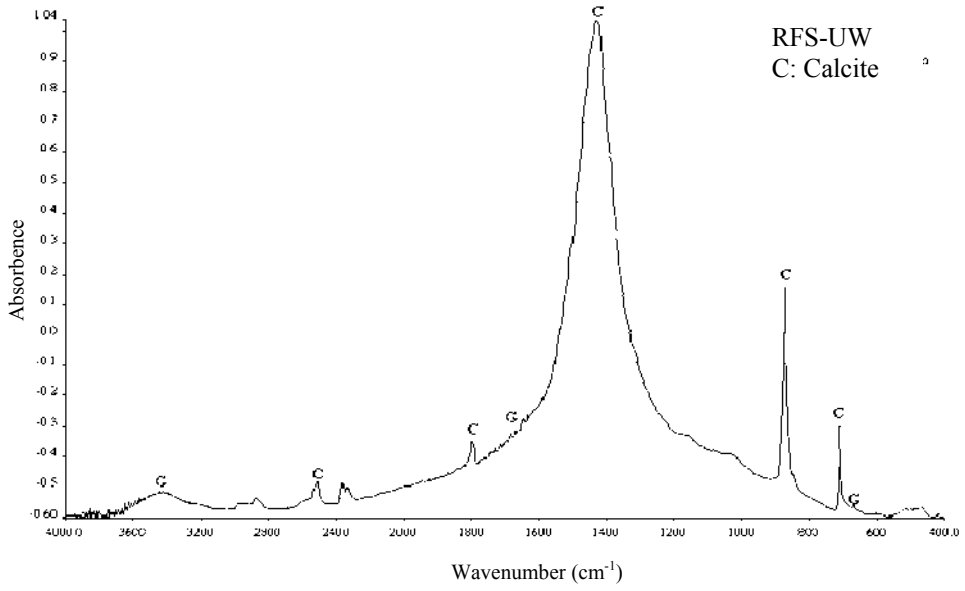

(a)

Figure 37. FT-IR graphs of Unweathered Layer of the samples (a): Roof Floor Sample (RFS-UW), (b): Fifth Floor Sample (FfFS-UW), (c): First Floor Sample (FsFS-UW)

(Continued on next page)

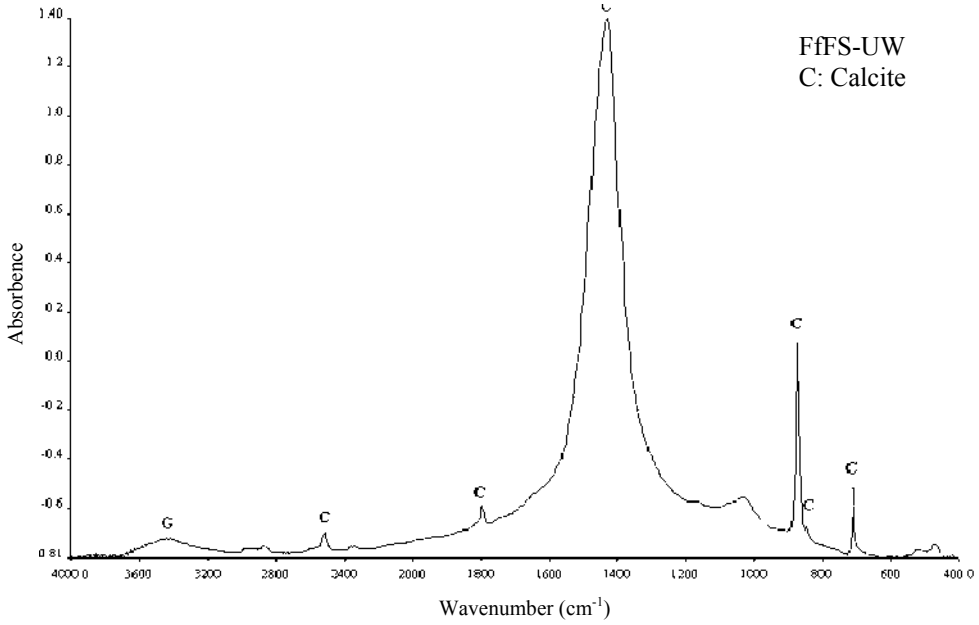

(b)

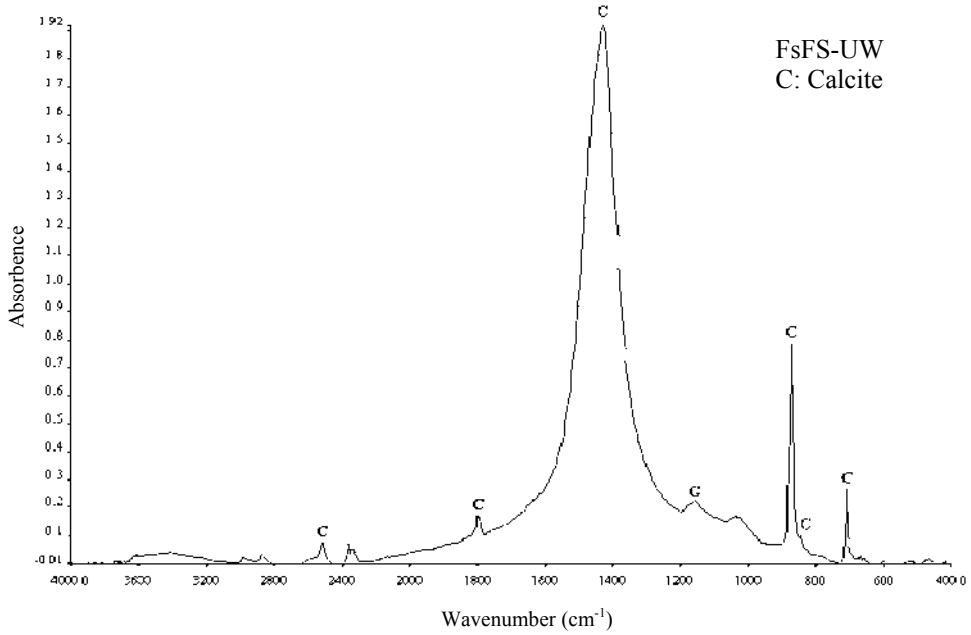

(c)

Figure 37. (Cont.)

3.3.2. Mineralogical Compositions of Limestone Affected from Air Pollution

Mineralogical compositions of the weathered and under weathered parts of the samples were analyzed by the X-ray diffraction analyses. The weathered parts of the samples were taken from the surfaces to the 5 mm inside of the limestone (Figure 38). The under weathered parts were taken from the 5-15 mm inside of the limestone (Figure 39). Gypsum and Calcite crystals were determined on the weathered and under weathered parts of the limestone. The existence of the gypsum proves the effects of air pollution. Formation of gypsum shows the reaction of calcium carbonate with the sulphure oxides (Montana et al. 2008).

At the weathered part of the Fifth Floor sample (FfFS-W1, FfFS-W2), gypsum was not detected in the XRD. It can be explained with its unsheltered location on the façade of the apartment. Because black crusts on the stone surfaces were wash out with rain water.

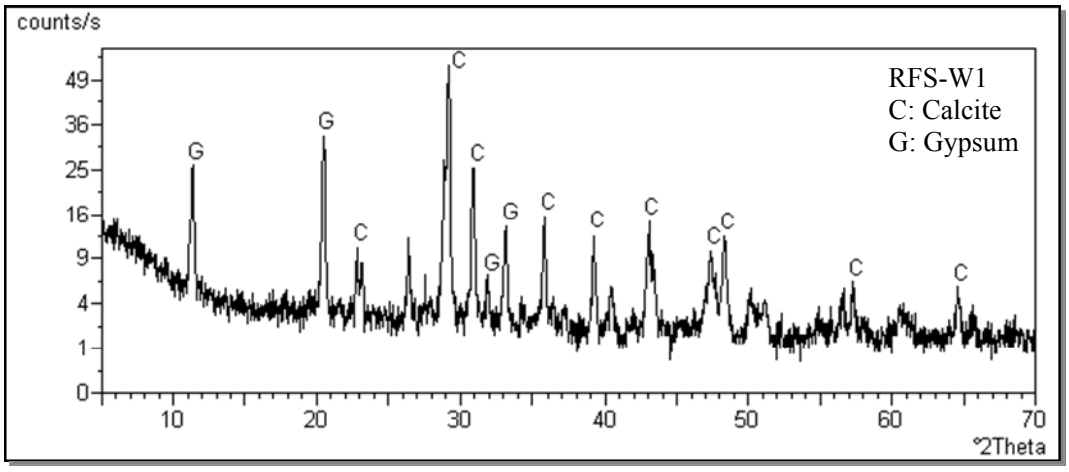

(a)

Figure 38. XRD patterns of the Weathered Layers (from surface to 5mm inner) of the samples (a): Roof Floor Sample (RFS-W1), (b): Fifth Floor Sample (FfFS-W1), (c): First Floor Sample (FsFS-W1)

(Continued on next page)

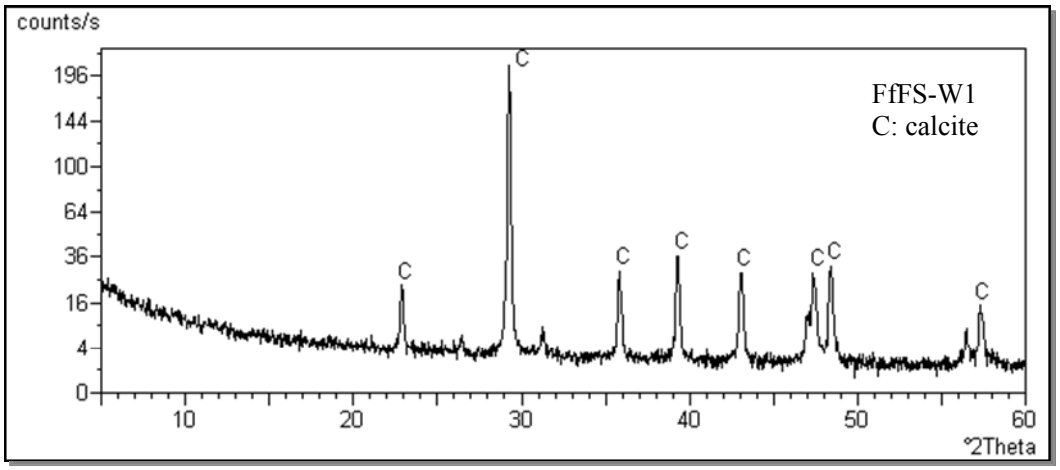

(b)

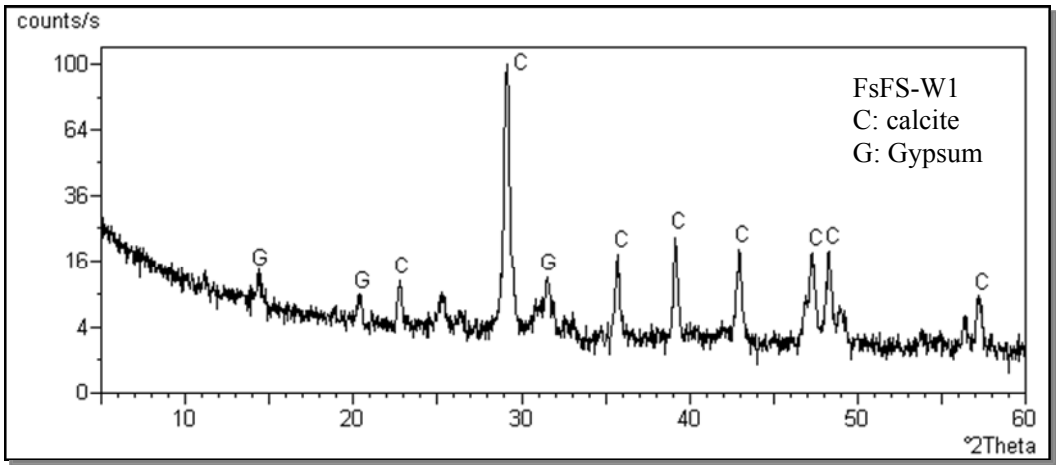

(c)

Figure 38. (Cont.)

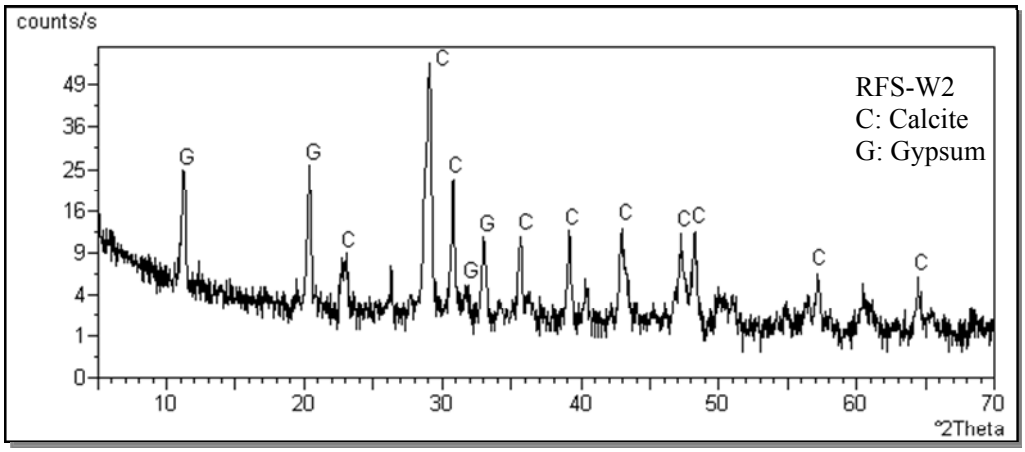

(a)

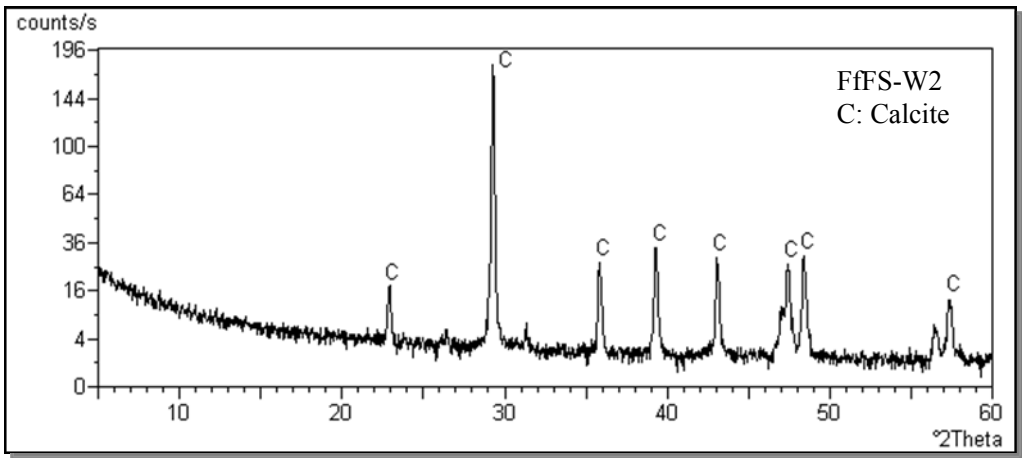

(b)

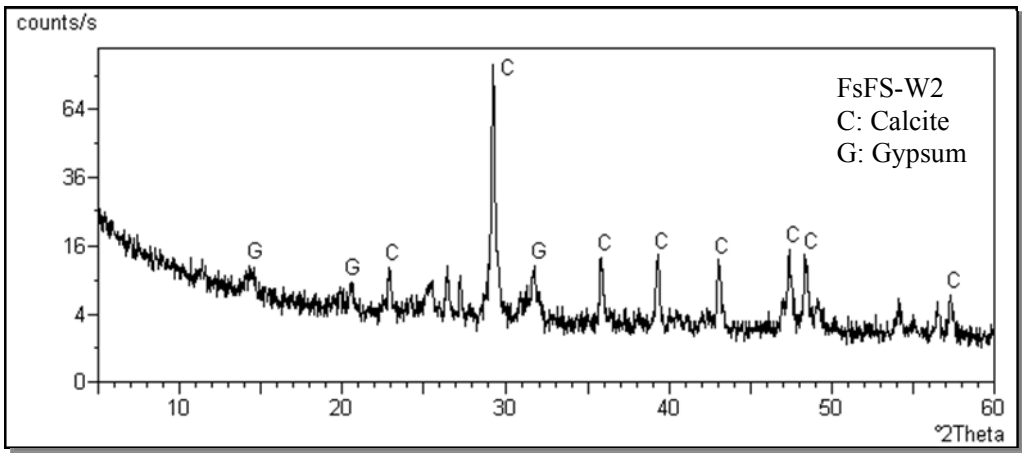

(c)

Figure 39. XRD patterns of the Weathered Layer-2 (approximately from 5mm to 15 mm inside) of the samples (a): Roof Floor Sample (RFS-W2), (b): Fifth Floor Sample (FfFS-W2), (c): First Floor Sample (FsFS-W2)

Mineralogical compositions of the weathered parts and under weathered parts of the collected samples were analyzed with FT-IR analysis. At the weathered parts, the the strong absorption bands of Gypsum at 3611 cm^{-1} , 1620 cm^{-1} , 1146 cm^{-1} , 1116 cm^{-1}, 1008 cm^{-1} ,661 cm^{-1} and 599 cm^{-1} were indicated at the roof floor and first floor samples. Also Quartz was observed in the FT-IR spectrum at 1094 cm^{-1} and 781 cm^{-1}. At fifth floor sample that taken from the unsheltered part of the façade quartz was not indicated and gypsum was observed at 3423 cm^{-1} (Figure 40).

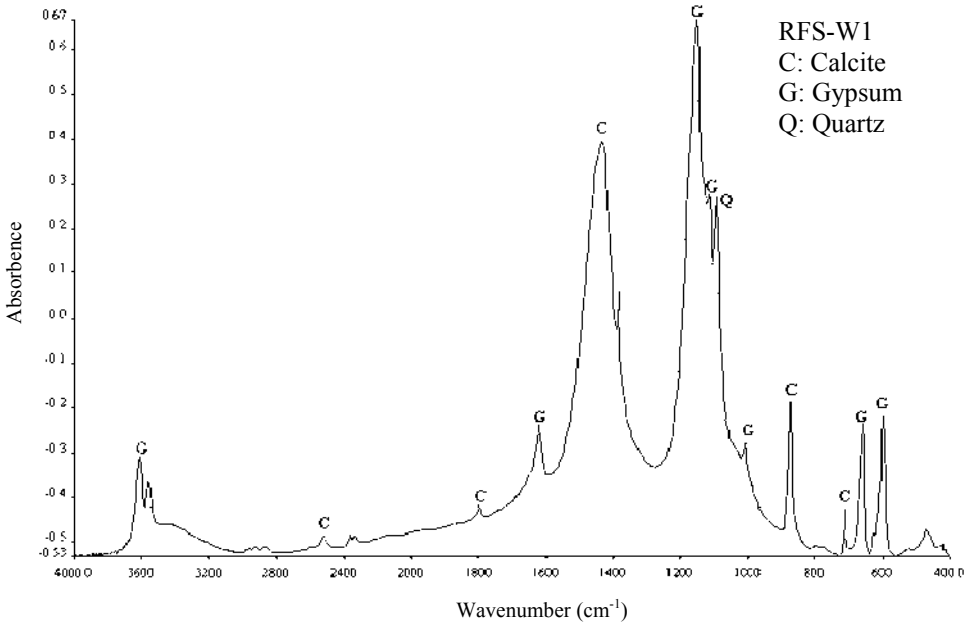

(a)

Figure 40. FT-IR graphs of the Weathered Layer-1 of the samples (A): Roof Floor Sample (RFS-W1), (B): Fifth Floor Sample (FfFS-W1), (C): First Floor Sample (FsFS-W1)

(Continued on next page)

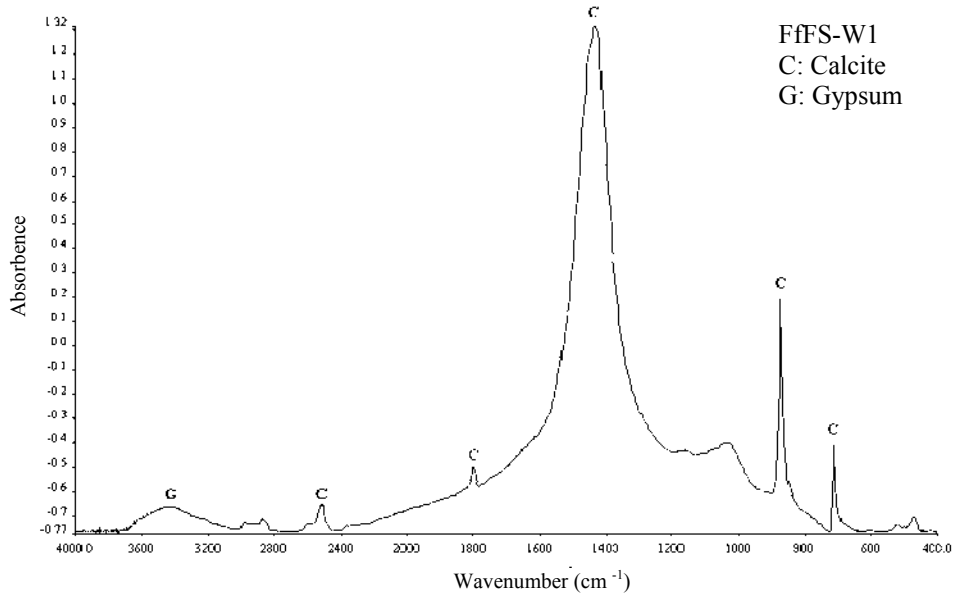

(b)

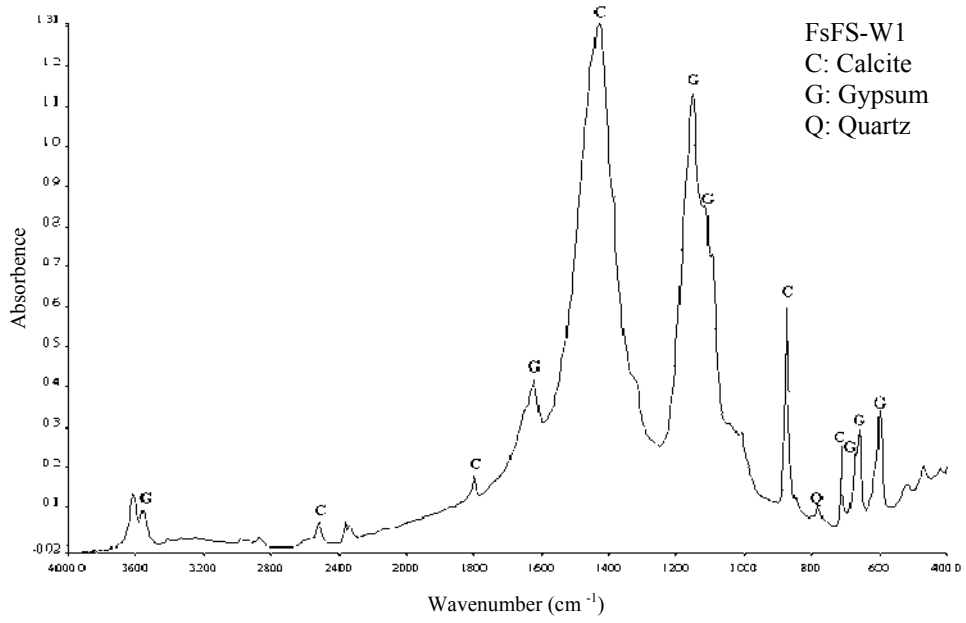

(c)

Figure 40. (Cont.)

At the under weathered parts (weathered layer-2) the FT-IR spectrum the strong absorption bands of Gypsum at 1152 cm^{-1} , 1095 cm^{-1} , 1008 cm^{-1} ,661 cm^{-1} and 599 cm^{-1} were indicated at the roof floor and first floor samples. Quartz was observed only at the first floor sample in the FT-IR spectrum at 781 cm^{-1}. At fifth floor sample that

taken from the unsheltered part of the façade gypsum was observed at 3423 cm^{-1} (Figure 41).

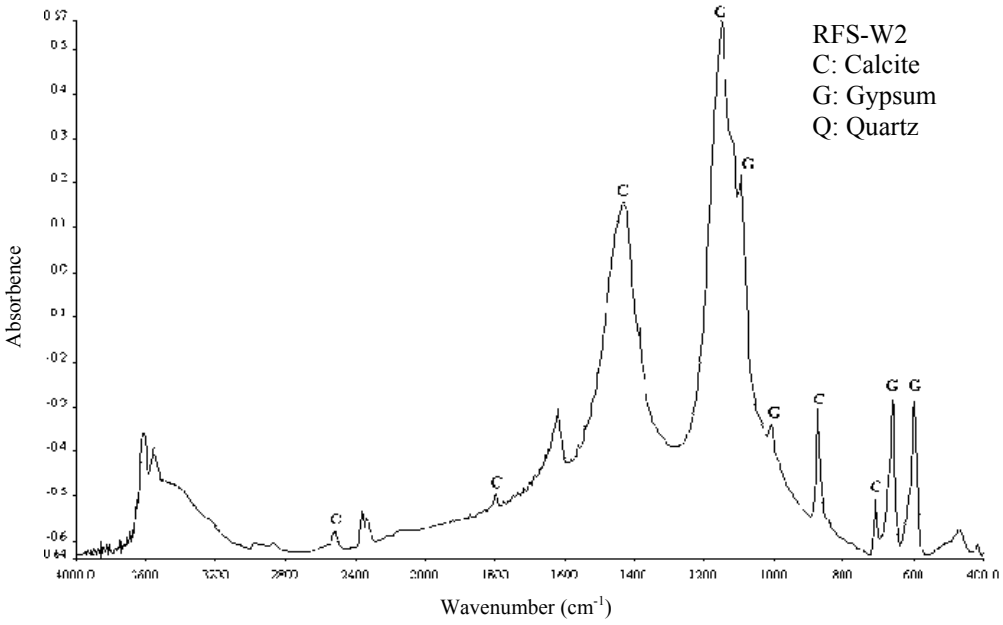

(a)

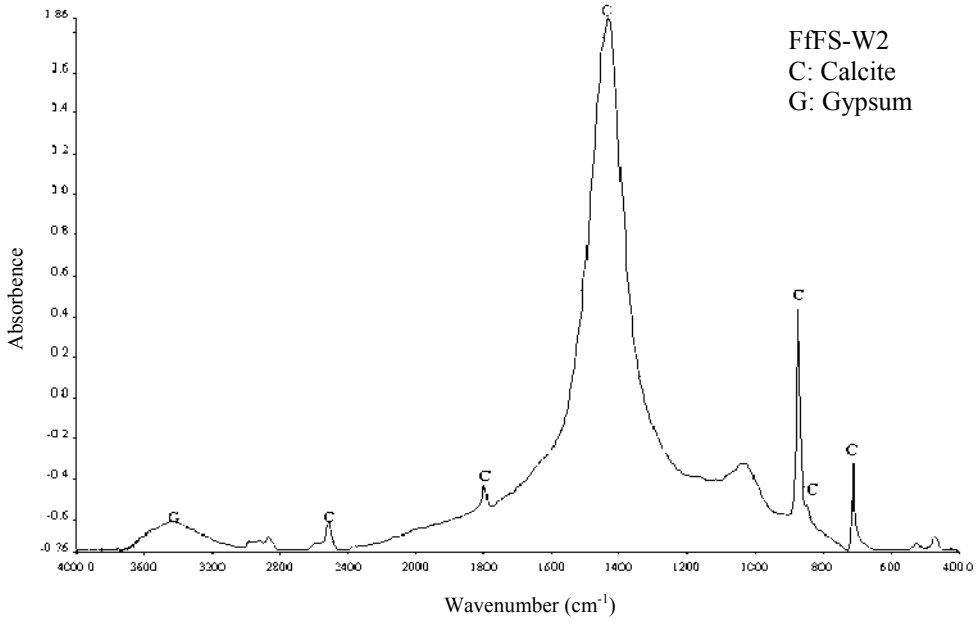

(b)

Figure 41. FT-IR graphs of the Weathered Layer-2 (approximately from 5mm to 15 mm inside) of the samples (A): Roof Floor Sample (RFS-W2), (B): Fifth Floor Sample (FfFS-W2), (C): First Floor Sample (FsFS-W2)

(Continued on next page)

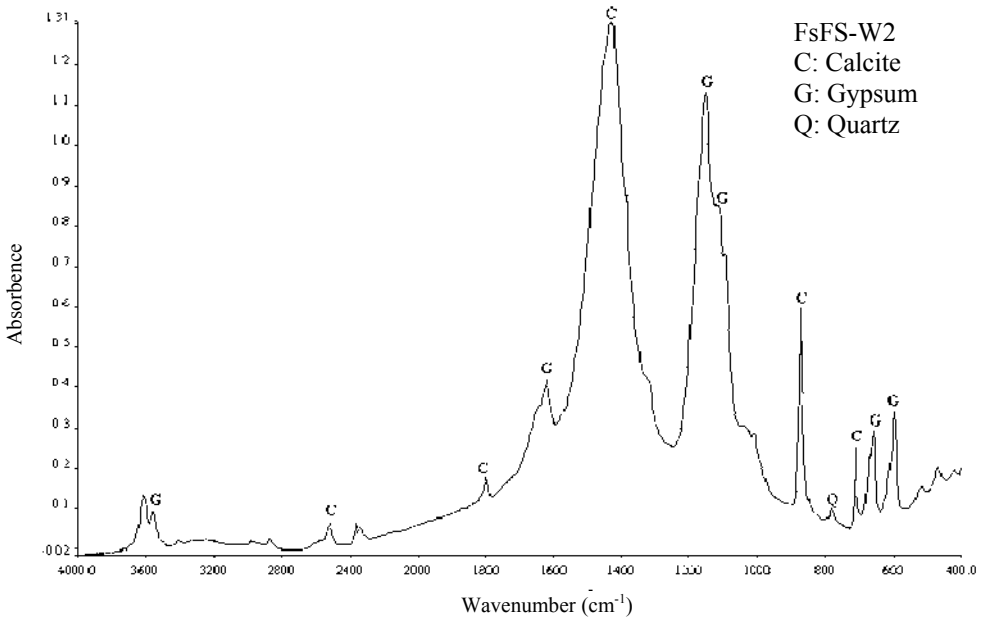

(C)

Figure 41. (Cont.)

3.4. Chemical Compositions of Unweathered and Weathered Samples

Chemical composition of limestone was determined by Scanning Electron Microscope (SEM-EDS) analysis. At the first floor sample (FsfS) three pellets were prepared from the weathered, under weathered and unweathered layers to analyze in SEM.

On the unweathered parts of the sample, calcium was found about 43 % and oxygen about 52%. On the weathered and under weathered parts, the percentage of Ca is decreased but S is increased due to the gypsum formation (Figure 42).

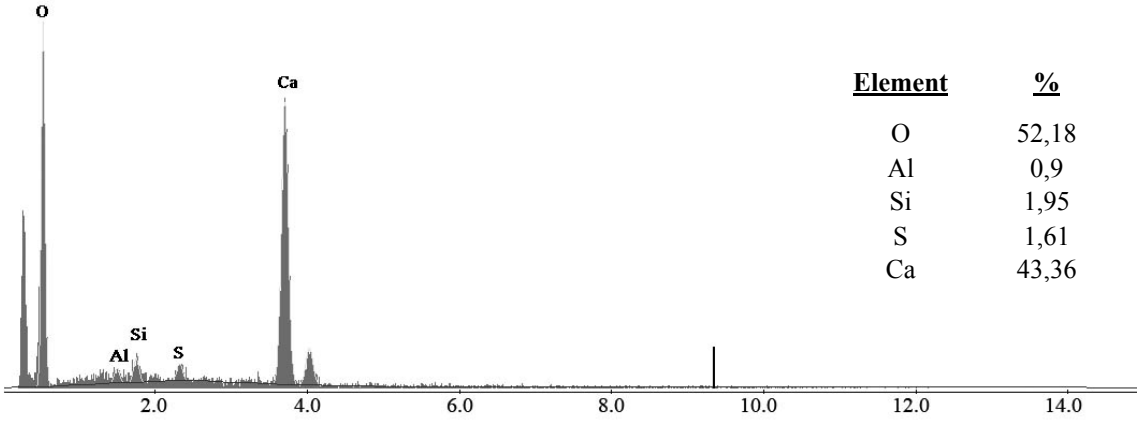

Element	%
O	52,18
Al	0,9
Si	1,95
S	1,61
Ca	43,36

(a)

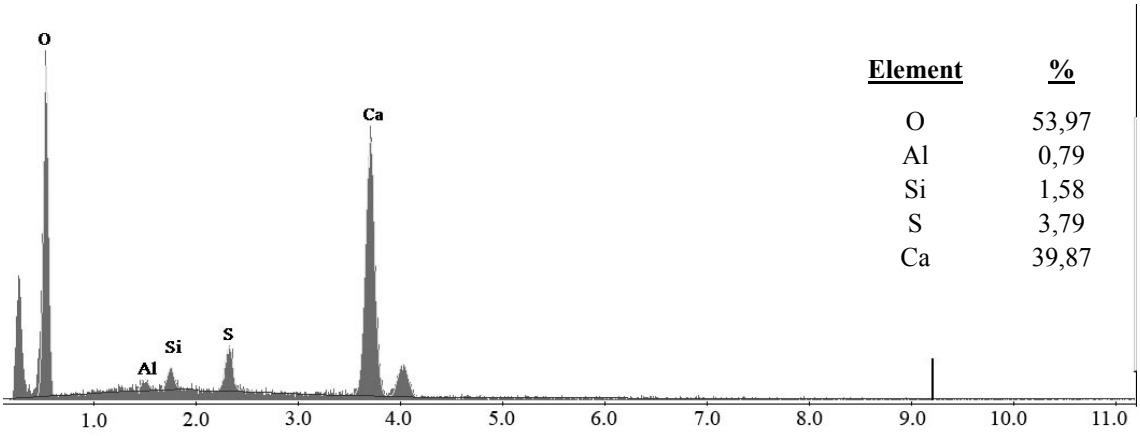

Element	%
O	53,97
Al	0,79
Si	1,58
S	3,79
Ca	39,87

(b)

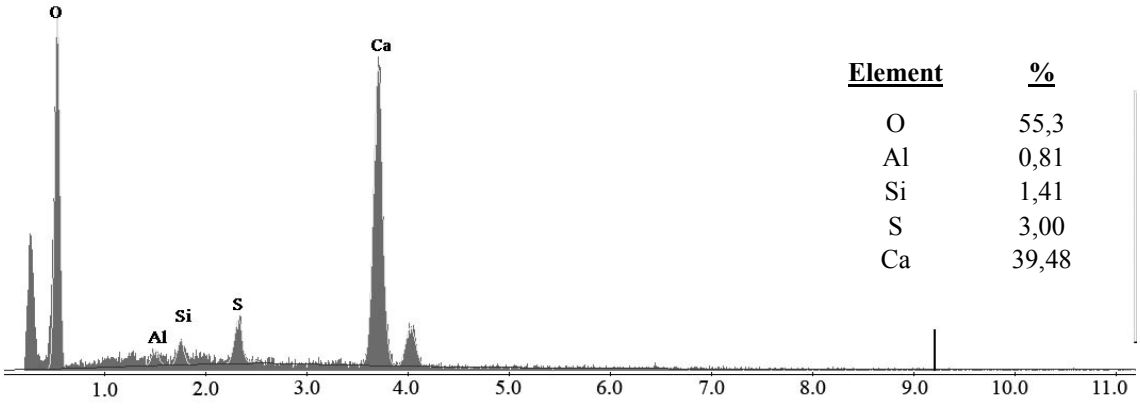

Element	%
O	55,3
Al	0,81
Si	1,41
S	3,00
Ca	39,48

(c)

Figure 42. EDX spectrum and chemical compositions of the First Floor Sample (a): Unweathered Layer, (b): Weathered Layer-1, (c): Weathered Layer-2 with matrix 256X200

The amount of gypsum was also determined on the cross section of the samples. The gypsum was observed from surface to inside the samples (~ 1 cm) (Figure 43).

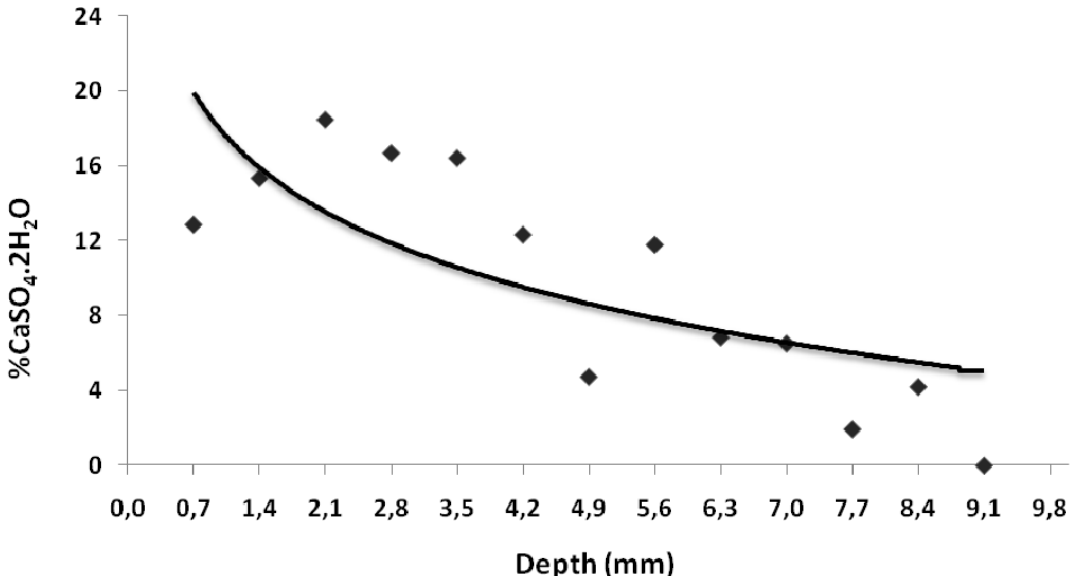

Figure 43. Gypsum rates of the FsFS from surface to the 9,8 mm inside.

As it seen in Figure 3.20, high amounts of gypsum are present on the surface and it decreases with dept of the sample. Gypsum that formed inside of the stone deteriorates the physical structure of the limestone (Figure 44).

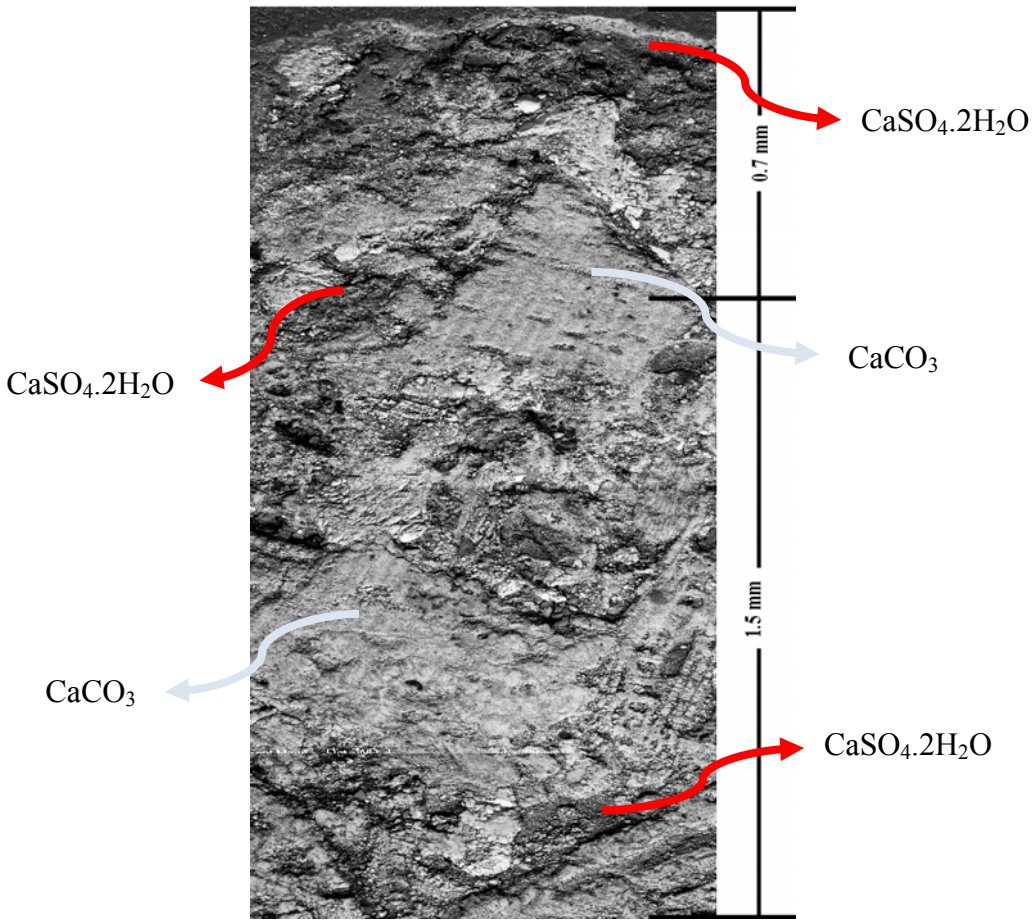

Figure 44. SE image of the FsFS from surface to the 2,2 mm inside showing the gypsum formation.

The chemical composition of the roof floor sample from surface to inside was also determined by SEM-EDS analyses (Table 4). As it is seen in Table 4 the high SO_3 concentration also was found on the surface of the samples. This can show the high amounts of gypsum formation on the limestone samples due to effects of SO_2.

Table 4. Table showing the amount of the elements in Roof Floor Sample (RFS)

Sample	CaO	SO_3	SiO_2	Al_2O_3	MgO	Na_2O	Cl_2O	Other
RFS-1	87,53	2,34	3,59	1,67	1,03	1,20	0,84	1,80
RFS-2	89,19	2,26	4,25	1,67	0,94	1,03	0,66	-
RFS-3	92,04	2,55	3,45	0,58	0,61	0	0,77	-
RFS-Average	89,58	2.38	3,76	1,30	0,86	0,74	0,75	0,60

Gypsum crystal ($CaSO_4.2H_2O$) at the Roof Floor sample was indicated by SEM analysis (Figure 45).

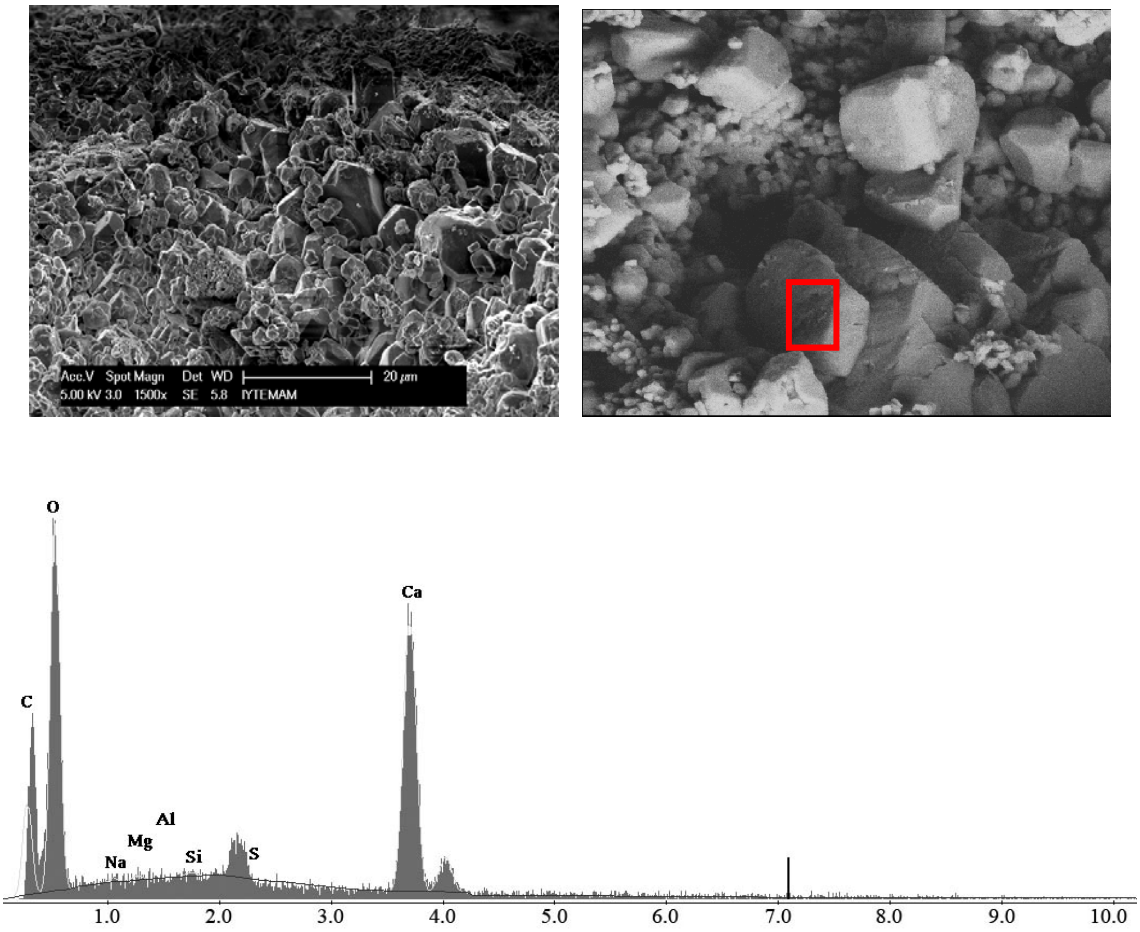

Figure 45. SE image and EDX spectrum of the gypsum crystals on the Roof Floor sample (RFS) with a magnification setting of 1500x and accelerating voltage 5 kV

SEM-EDS analyses show that surface of the samples are composed of mainly Ca and S originated from gypsum formation and Na, Si, Al, Mg and Cl originated from deposited airborne particles on the surfaces and sea salts. The existence of Na and Cl can be related to the contribution of the salt and the existence of Al and Si can be related to crustal elements.

% Ca, S, Na, Cl, Si, Al and Mg values distribution in the First floor sample (FsF-St) were determined with SEM - EDS from surface to the inner in 9.8 mm distance. The existence of these elements could be used as an indicator of deterioration (Videla, et al.

2000). These elements have accelerating effects on the biodeterioration of stone (Nuhoğlu, et al. 2006).

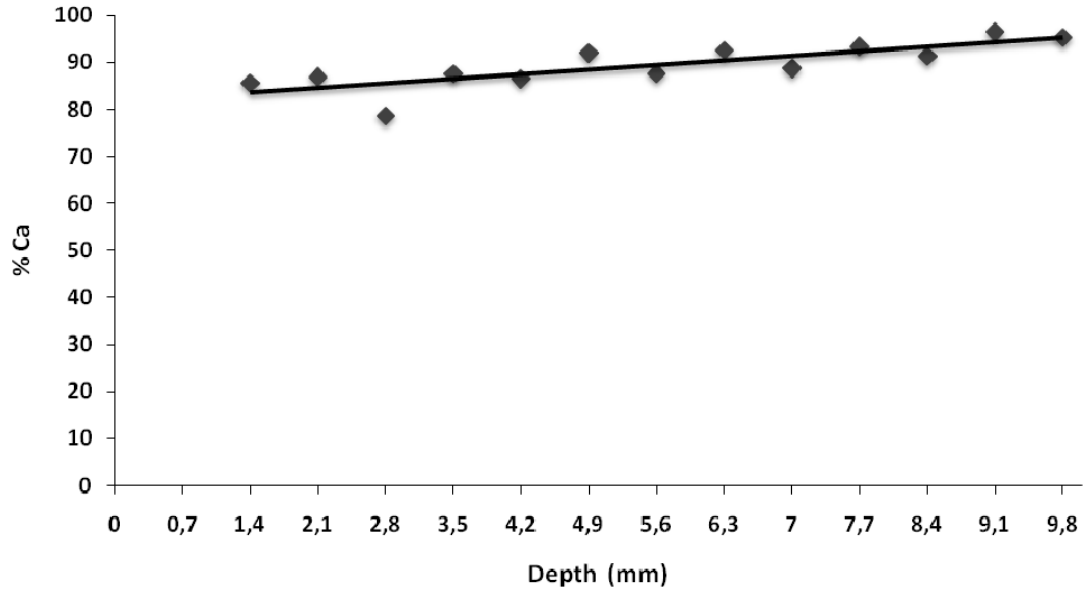

Figure 46. % Ca value from surface to the 9.8 mm inner in the sample of First Floor (FsFS)

In the Figure 46, % Ca in the stone is increased from surface to the inner parts due to the conversion of calcium carbonate ($CaCO_3$) to gypsum ($CaSO_4.2H_2O$). Sulphure dioxide reaches to the stone surface by wet and dry deposition and penetrates to the inside of the stone. As a result, gypsum crystals on surface of the stone (RFS) were observed in SEM-EDS analyses (Figure 47). It is seen in Figure 48 that the sulphur formation advances towards the inner parts of the stone approximately 1cm from the surface. When sulphure dioxide reacts with calcite and this reaction leads to significant structural damage due to the changes in mineral volume associated with gypsum-calcite transition (Lefévre and Ausset 2002).

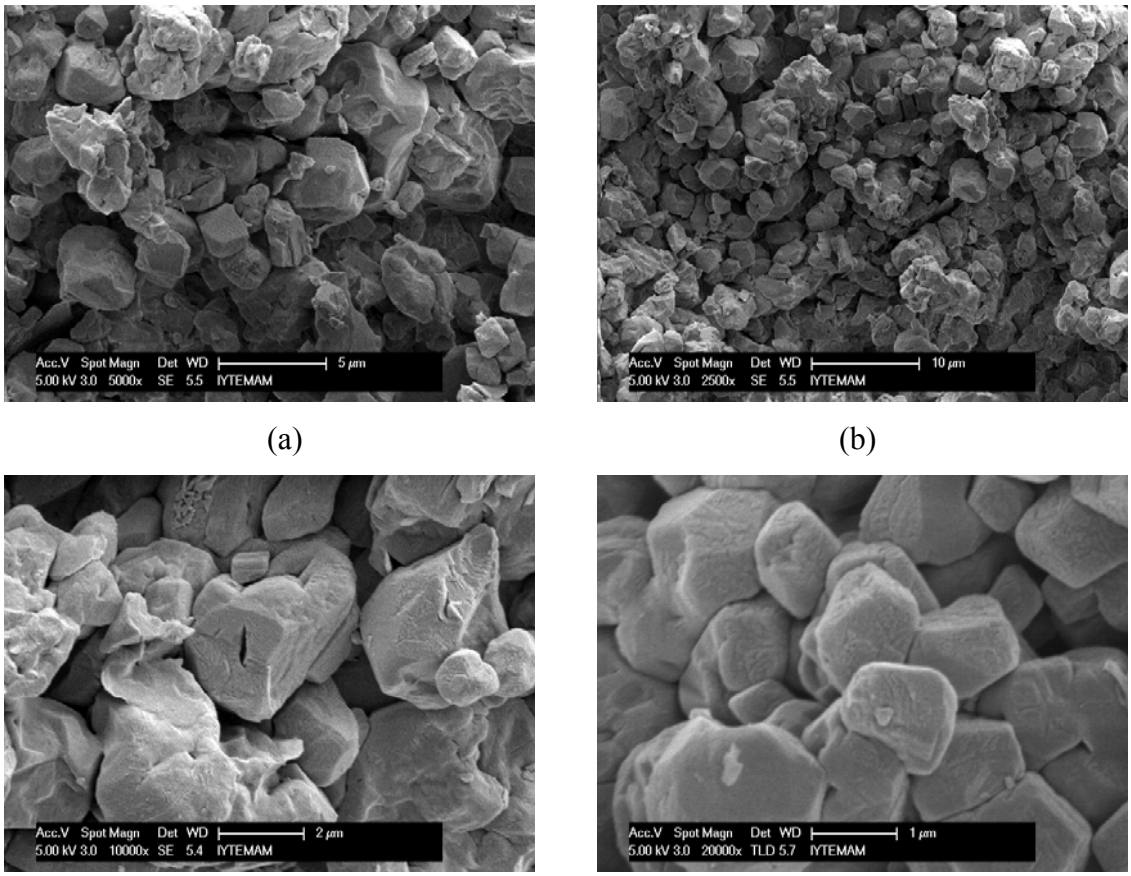

(a) (b)

(c) (d)

Figure 47. SEM images of gypsum crystals at Roof Floor Sample (RFS) with a magnification setting of (a) 5000 x, (b) 2500 x, (c) 10000 x and (d) 20000 x and accelerating voltage 5 kV

Similar study about the sulphure concentration (%) profiles was studied by Lefévre and Ausset (2002). They studied a known stone sample until reaching the unsulphated sound substrate that exposed on different sites during time periods. Mostly exposed sample was about 83 years and the sulphure concentration value reached the unsulphated sound in 1.6 – 1.8 mm. When it compared with the sample of Botter Apartment, intense weathering is easily observed. At the first floor sample (FsFS) unsulphated sound was reached in 9.1 - 9.8 mm that is the six times more than the sample of Ausset's study. It can be explained high amount of air pollution in the site and the longer the exposure time (Lefévre and Ausset 2002).

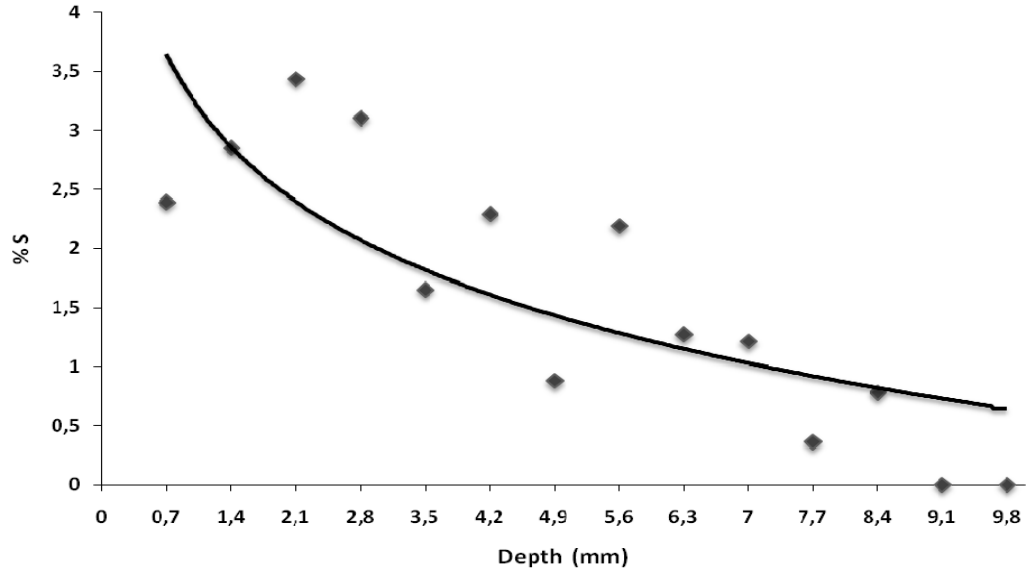

Figure 48. % S value from surface to the 9.8 mm inner in the sample of First Floor (FsFS)

In the composition of the limestone, chlorides present at the level of 1 % that mainly dependent on the deposition of marine sediments (Fassina et al. 2002). The high level of the Cl (Figure 50) element in the weathered sample can be attributed to the essence of salt that deposited from the sea spray. With the essence of salt the rates of Na (Figure 49) element show similarity with Cl element due to sea spray.

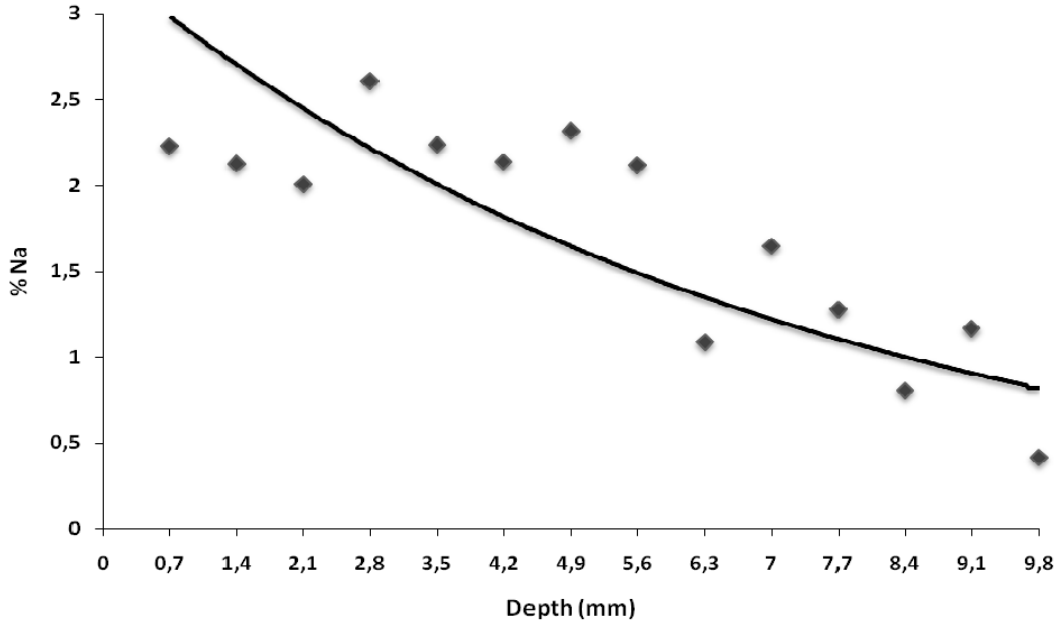

Figure 49. % Na value from surface to the 9.8 mm inner in the sample of First Floor (FsFS)

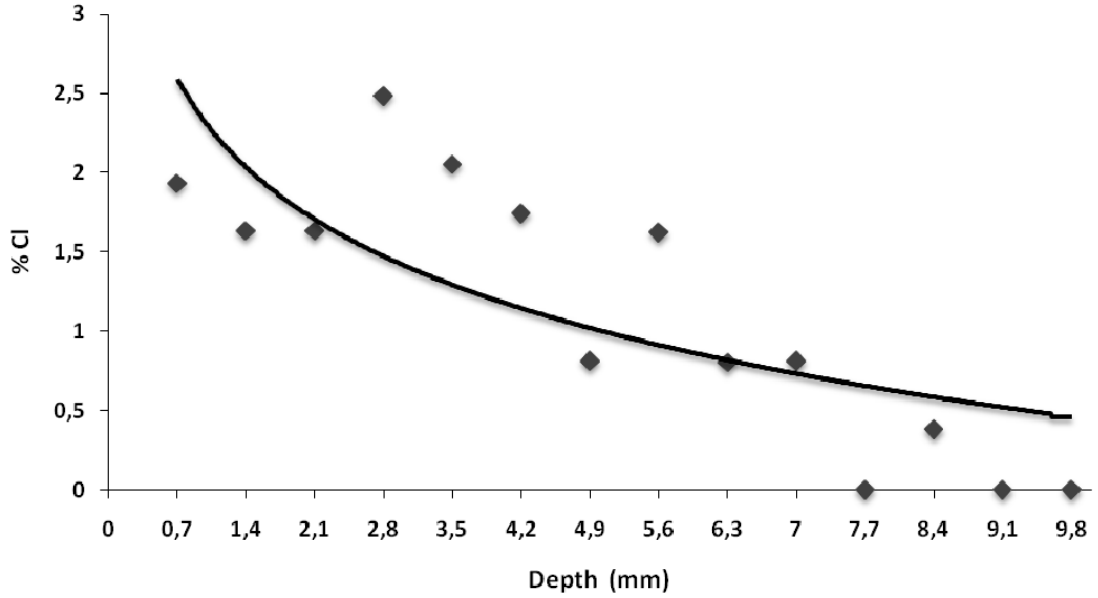

Figure 50. % Cl value from surface to the 9.8 mm inner in the sample of First Floor (FsFS)

The other elements that increased with the affect of air pollution are silicon, aluminum (Figure 51) and magnesium (Figure 53). The silicon (Si) (Figure 52) is originated from quartz and clay particles (Török et al. 2006).

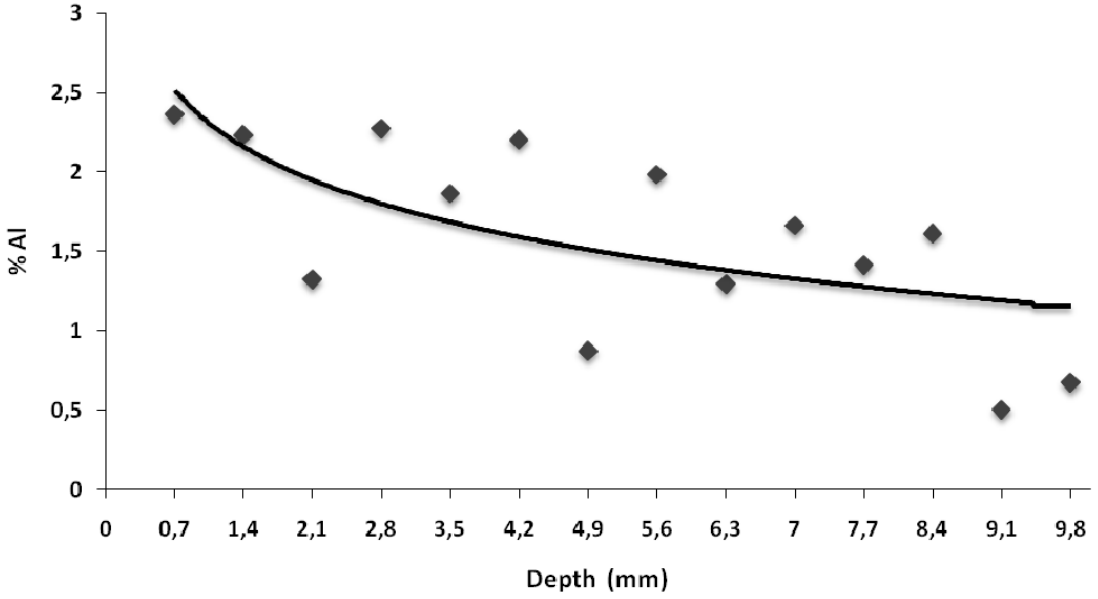

Figure 51. % Al value from surface to the 9.8 mm inner in the sample of First Floor (FsFS)

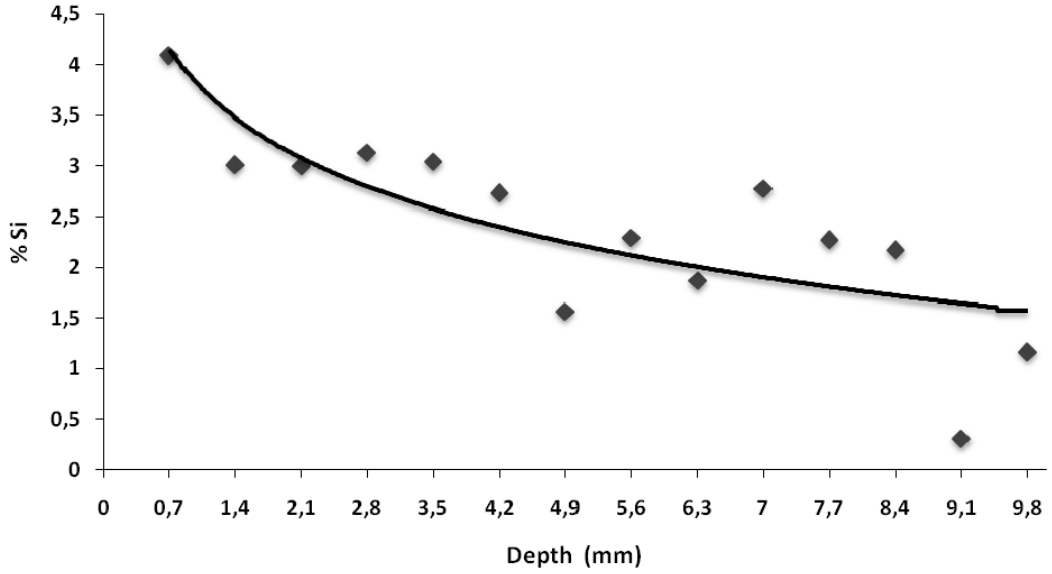

Figure 52. % Si value from surface to the 9.8 mm inner in the sample of First Floor (FsFS)

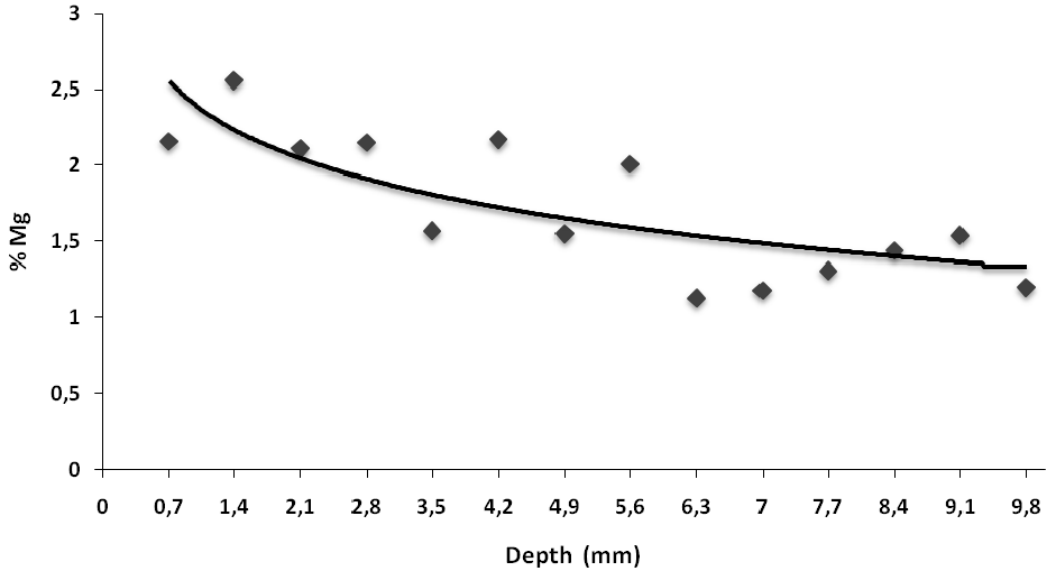

Figure 53. % Mg value from surface to the 9.8 mm inner in the sample of First Floor (FsFS)

3.5. Determination of Weight Loss of Samples by Thermogravimetric Analysis

In order to quantify the gypsum formation on the samples Thermogravimetric analysis (TGA) was carried out. At the weathered layers of the Roof floor and First floor samples the weight losses were around 32-34 % due to the high amounts of gypsum formation. However on the unweathered layer of the roof floor, the weight loss

is around 42% due to high amounts of calcite. In the Table 5 % weight loss of the samples were given at the different range of temperatures.

Table 5. TGA analysis showing the % weight loss of samples between the different range of temperatures

	25 - 100 C^0	100 - 170 C^0	170 - 250 C^0	250 - 550 C^0	550 - 1000 C^0
RFS- Weathered Layer-1	1,23371	9,53385	0,67695	3,12932	16,86720
RFS-Unweathered Layer	0,20039	0,17615	0,11810	1,04652	42,76320
FsFS-Weathered Layer-1	1,27800	3,48126	0,64943	5,27969	22,27263
FfFS- Weathered Layer-1	0,33925	0,21040	0,16983	1,55646	39,45127

In this study, adsorbed water was determined by weight loss of samples at temperatures between 25–100 ^{0}C. At the weathered layer of the Roof Floor sample (Figure 54) the adsorbed water was found in the range about 1 %. Gypsum formation on the weathered layer of the Roof Floor sample can be determined by weight loss of bound water of gypsum at temperature between 100 – 250 ^{0}C. The dehydration of gypsum takes place in two next stages (3.1 and 3.2) (Montoya, et al. 2004);

$$CaSO_4.2H_2O \rightarrow CaSO_4.\ ½\ H_2O + 3/2\ H_2O \quad (3.1)$$

$$CaSO_4.\ ½\ H_2O \rightarrow CaSO_4 + ½\ H_2O \quad (3.2)$$

The weight loss observed at temperature between 100-250 ^{0}C was about 10 %. Organic matter originated from air pollution was determined by weight loss of sample at temperature between 250-550 ^{0}C. The organic matter was found around 3%. Percentage of calcium carbonate content of weathered layer of the roof floor sample was found by weight loss of sample at temperature between 550-1000 ^{0}C. The calcinations of calcite express with following equation (3.3);

$$CaCO_3 \rightarrow CaO + CO_2 \quad (3.3)$$

The weight loss observed at temperature between 550-1000 ^{0}C was about 16 %. This means that large amount of calcium carbonate ($CaCO_3$) was converted into gypsum ($CaSO_4.2H_2O$) by the effects of air pollution.

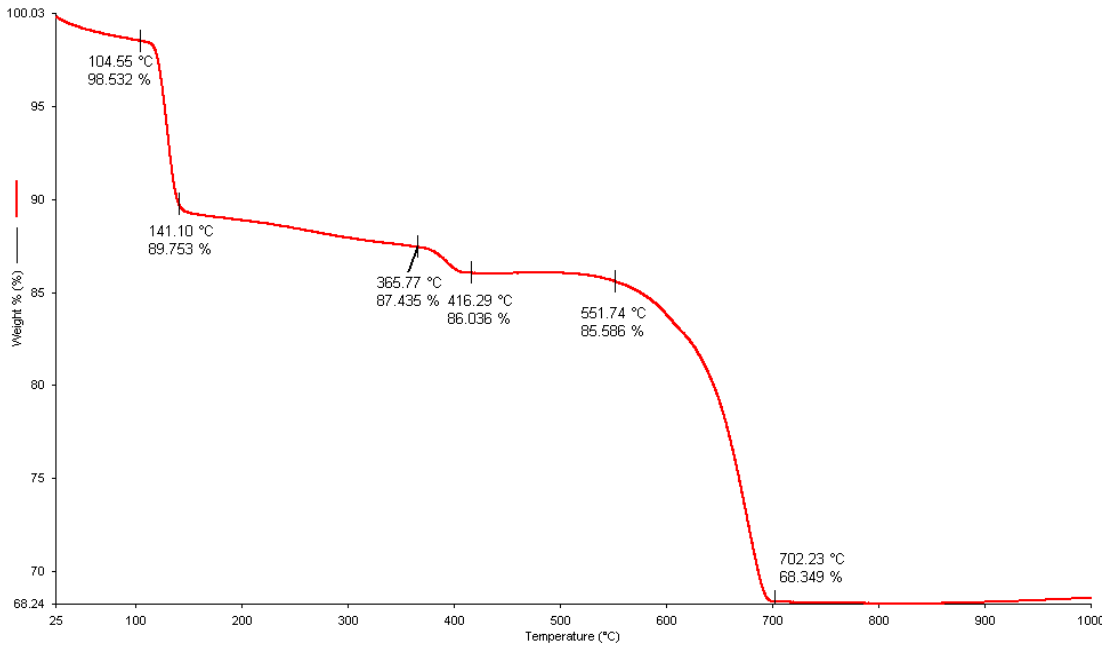

Figure 54. TGA analysis of RFS-Weathered Layer-1

Percentage of calcium carbonate content of unweathered layer of roof floor sample was determined by TGA analysis (Figure 55). TGA analysis shows that calcination of unweathered limestone was started at temperature 560 ^{0}C and completed at around 750 ^{0}C. The weight loss observed at these temperatures was found about 42%.^{0}C.

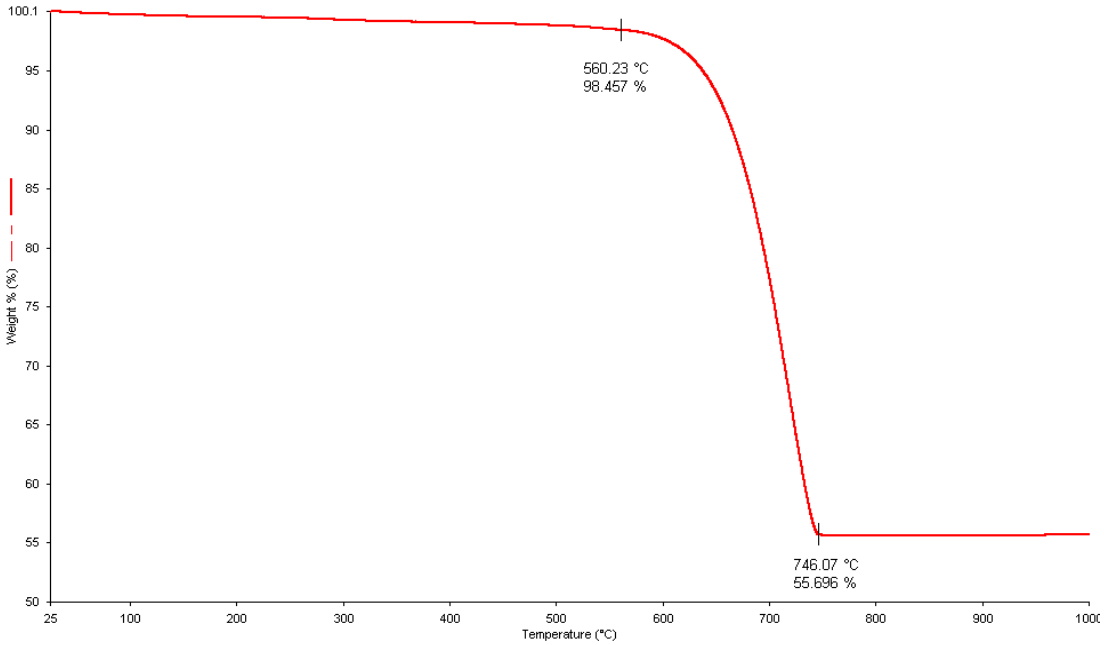

Figure 55. TGA analysis of RFS-Unweathered Layer

At the weathered layer of the First Floor sample (Figure 56) the adsorbed water was found in the range about 2 %. Bound water of gypsum was determined at temperature between 100-250 ^{0}C was about 4 %.

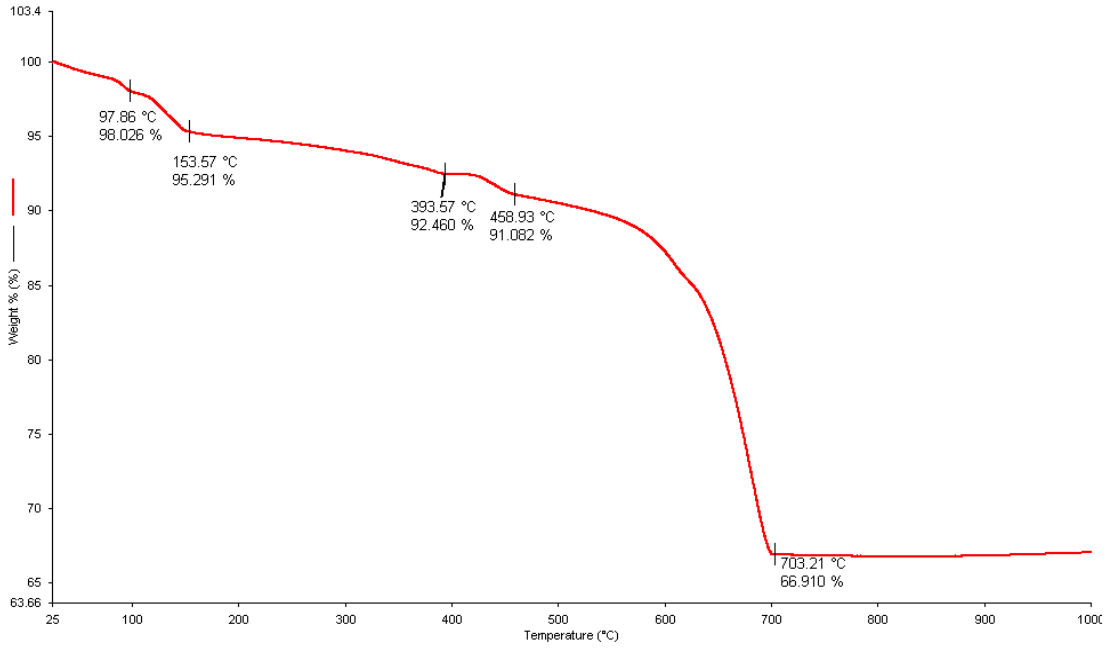

Figure 56. TGA analysis of FsFS- Weathered Layer-1

Organic matter originated from air pollution at weathered layer of the first floor sample was determined at temperature between 250-550 ^{0}C. The organic matter weight was found around 6%. Calcium carbonate content of weathered layer of first floor sample was found by weight loss of sample at temperature between 550-1000 ^{0}C. The weight of the calcium carbonate content was around 23 %. Thermogravimetric analyses of the weathered layers show that more amount of calcium carbonate was converted into the gypsum at the first floor sample.

Weathered layer sample of the fifth floor was taken from the unsheltered place of the façade. The TGA analysis results of weathered layer of the fifth floor sample (Figure 57) show similarities with the unweathered sample. Gypsum easily dissolves with rain water and causes erosion on the stone surface. This leads an open new surface that ready for new gypsum formations. Calcination of weathered layer of the fifth floor sample was started at temperature 560 ^{0}C and completed at around 750 ^{0}C. The weight loss observed at these temperatures was found about 39%.

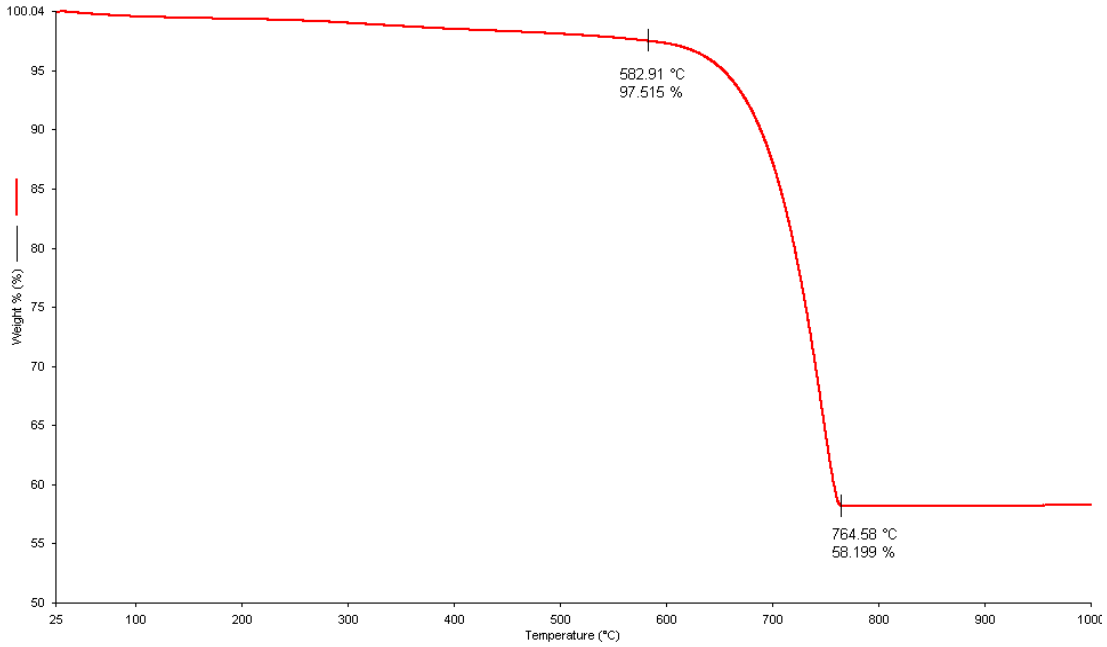

Figure 57. TGA analysis of FfFS- Weathered Layer-1 (the sample which taken from the unsheltered place)

CHAPTER 4

CONCLUSION

In this study, air pollution effects on limestone used in the construction of façade of historic Botter Apartment in İstanbul has been examined. For this purposes physical, mineralogical and chemical compositions of weathered limestone were determined by XRD, SEM-EDS, FT-IR and TGA analyses.

Determination of weathering forms occurred due to air pollution on the stone surfaces is a crucial stage in order to propose preservation treatments and convenient intervention methods for conservation works of the monument.

In the context of this study, the laboratory works that were carried out in order to determine the structure of the limestone demonstrated that the sound part of the limestone is low dense and high porous. It consists of calcite crystals with sea shells and corals.

The main effect of air pollution on limestone in İstanbul is gypsum formation due to the effect of sulphure dioxide (SO_2). Sulphure dioxide reaches to the stone surface together with other pollutants by wet and dry deposition. Gypsum formation on limestone surfaces unsheltered from rain is mainly by wet deposition process. On sheltered surfaces of limestone, gypsum formation proceeds as black crust formation due to the dry deposition. Condensation may also play an important role in gypsum formation on such sheltered surfaces together with dry deposition.

The gypsum formation is not restricted to the surface of the stone. Deeper penetration and absorption of sulphure dioxide is observed in limestone because of their more porous structure.

In İstanbul average daily temperature are low and average relative humidity and sulphure dioxide concentrations are high in winter time. The results of this study indicates that İstanbul atmosphere, with its coinciding high relative humidity and sulphure dioxide concentrations in winter times is in favor of gypsum formation on limestone.

It was determined that gypsum formation not only occurred on the surface of the stone but it was also penetrated into 1.5 cm inside. High amount of gypsum was

calculated on the basis of TGA results. Thus, it was indicated that basic physical and chemical structure of the stone was changed drastically.

The façade of Botter Apartment was built up from rich decorated limestone that reflect the characteristics of its era. Since these ornamentations were subjected to less rain water, much more gypsum formation was observed in these parts. Besides this, rain water leads to back weathering due to the loss of black crust on the parts which are exposed to direct rain water.

Cleaning of deteriorated stone surfaces causes to reveal of unweathered stone surfaces which will be deteriorated because of the air pollution. Cleaning works should be maintained after air pollution which threatens the historical monuments is decreased. Before cleaning, consolidation of surface structure should be implemented.

Consolidation of the surface with a biodegradable polymer might be a suitable method to prevent the surface (Ocak et al. 2009). Biodegradable polymers have two fundamental properties that are required for conservation of historical buildings. Biodegradable polymers employed, which form a protective barrier against water and SO_2, should be reversible and should enable to further interventions.

Recently, it is obvious that air pollution could not be disappeared in a short time. Because of that, consolidation on stone surfaces is strongly recommended urgently.

REFERENCES

Air Pollution Forecasting Service. 2010. http://airpol.fatih.edu.tr/istanbul.php. (accessed May 30, 2010).

Alessandrini, G., Toniola, L., Antonioli, A., Silvestro, A.D., Piacenti, F., Ponticelli, S.R. and Formica, L. 1993. *On the Cleaning of Deteriorated Stone Minerals, Conservation of Stone and Other materials*. Proceedings of the International RILEM/UNESCO Congress: 503-511

Atlas, R. M., Chowdhury, A.N. and Gauri, K. L. 1988. Microbial Calcification of Gypsum-rock and Sulfated Marble. *Studies in Conservation*: 149-153

Batur, A. 2005. "Art Nouveau Mimarlığı ve İstanbul", Ed. Salman, Y. *Avrupa'dan İstanbul'a Yeni Sanat 1890-1930, Art Nouveau from Europe to İstanbul 1890-1930*. Sean Ofset. İstanbul: 141-166

Batur, A. 1993. "Botter Apartmanı". *Dünden Bugüne İstanbul Ansiklopedisi*. Ana Basım AŞ. 2: 312-314

Batur, A. 1993. "Art Nouveau". *Dünden Bugüne İstanbul Ansiklopedisi*, Ana Basım AŞ. 1: 327-333

Bityukova, L. 2006. Air Pollution Effect on the Decay of Carbonate Building Stones in Old Town of Tallinn. *Water Air and Soil Pollution*. 172: 239-271

Bonazza, A., Messina, P., Sabbioni, C., Grossi, C. M. ans Brimblecombe, P. 2009. Mapping the Impact of Climate Change on Surface Recession of Carbonate Buildings in Europe. *Science of the Total Environment*. 407 (6): 2039-2050

Böke, H., Caner-Saltık, E. N. and Göktürk, H. 1992. Gypsum Formation on Traveertines in Polluted Atmosphere. *7th International Congress on Deterioration and Conservation of Stone*. Proceedings J. Delgado Rodriques Ed. Laboratorio Nacional de Engenharia Civil. Lisbon, Portugal. 1: 237-246

Böke, H., Gauri, K. L. 2003. "Reducing Marble-SO_2 Reaction Rate by the Application of Certain Surfactants". Water Air and Soil Pollutuion. Vol. 142, pp. 59-70

Böke, H., Göktürk, H., Caner - Saltık E.N. and Demirci, Ş. 1999. Effect of Airborne Particles on SO_2 – Calcite Reaction. *Applied Surface Science*. 70-82

Böke, H., Göktürk, H. and Caner - Saltık E.N. 2002. Effect of Some Surfactants on SO_2-Marble Reaction. *Materials Letters*. 57: 935-939

Camuffo, D., Pagan, E., Del Monte, M., Lefevre, R. A. and Ausset, P. 2006. Modeling the Penetration of SO_2 within the Pores of Calcareous Stones and the Concentration of Gypsum in the Near Surface Layer. In *Heritage, Weathering and Conservation Vol.1 and Vol.2*. Proceedings and Monographs in Engineering. *Water and Earth Sciences*: 435-440

Cheng, J.R., Hwu, R., Kim, J.T. and Leu, S.M. 1987. Deterioration of Marble Structures. *Analytical Chemistry*. 59: 104-106

Charola, A. E., Ware, R. Acid Deposition and the Deterioration of Stone: a Brief Review of a Broad Topic. Ed. Siegesmund, S., Weiss, T. and Vollbrecht, A. 2002. *Natural Stone, Weathering Phenomena, Conservation Strategies and Case Studies*. The Geological Society. London. Special Publication no. 205: 393-406

Cimitan, L., Rossi, P.P. and Torraco, G. 1994. Accelerated Sulphation of Calcareous Materials in a Climatic Chamber: Effect of Protective Coatings and Inhibitors. *Proceedings of the 3rd International Symposium on the Conservation of Monuments in the Mediterreanen Basin*. Venice, İtaly. pp. 233-239

Çevresel Etki Değerlendirmesi ve Planlama Genel Müdürlüğü. 2010. http://www2.cedgm.gov.tr/icd_raporlar/istanbulicd2008_2009.pdf . (accessed May 30, 2010).

Çınar, K., Koçu, N. and Koç, İ. 1999. The Negative Effects of the Environment on Historical Monuments in Konya (Turkey). *Fresenius Environmental Bulletin*. 8(5-6): 236-242

Degan, G. A., Lippiello, D. and Pinzari, M. 2006. Air Pollution Modelling in an Italian Limestone Quarry: An ISO Simple Procedure in Forecasting PM 10 Dispersion. In *Safety and Reliability for Managing Risk Vol.1-3*. Proceedings and Monographs in Engineering. *Water and Earth Sciences*: 2217-2223

Delalieux, F., Cardell-Fermandez, C., Torfs, K., Vleugels, G. and Van Grieken, R. 2002. Damage Functions and Mechanism Equations Derived from Limestone Weathering in Field Exposure. *Water Air and Soil Pollution*. 139(1-4): 75-94

Diana, M., Gabrielli, N. and Ridolfi, S. 2007. Sulfur Determination on Stone Monuments with a Transportable EDXRF System. *X-Ray Spectrom Wiley InterScience.* 36: 424-428

Fassina, V. 1988. The Deterioration & Conservation of Stone, Studies and Documents on Cultural Heritage. *UNESCO – 1988*.

Fassina, V., Favaro, M. and Naccari, A. Principal Decay Patterns on Venetian Monuments. Ed. Siegesmund, S., Weiss, T. and Vollbrecht, A. 2002. *Natural Stone, Weathering Phenomena, Conservation Strategies and Case Studies*. The Geological Society. London. Special Publication no. 205: 381-391

Fresenius Environmental Bulletin. 2002. The Effects of Air Pollution on Carbonate Stone Monuments in Urban Areas (Sivas, Turkey). 11(8): 505-509

Gauri, K. L. and Bandyopadhyay, J. K. 1999. Carbonate Stone Chemical Behaviour, Durability, and Conservation. A Wiley-Interscience Publication John Wiley & Sons Inc. Canada.

Gauri, K.L., Doderer, G.C., Limscomp, N.T. and Sarma, A.C. 1973. Reactivity of treated and untreated Marble Specimens in an SO_2 Atmosphere. *Studies in Conservation*. 18: 25-35

Gauri, K.L., Popli, R. and Sarma, A.C. 1982/1983. Effect of relative humidity and grain size on the reaction rates of marble at high concentration of SO_2. *Durability of Building Materials*. 1: 209-216

Göktürk, H., Volkan, S. and Kahveci, S. 1993. Sulfation Mechanisms of Travertines: Effects of SO2 concentration, Relative Humidity and Temperature. Conservation of Stone and Other Materials. RILEM. Paris-Fransa.

Grelk, B., Christiansen, C., Schoouenborg, B. and Malaga, K. 2007. Durability of Marble Cladding – A Comprehensive Literature Review. American Society for Testing and Materials Special Technical Publication. *Dimension Stone Use in Building Construction*. 1499: 105-123

Grossi, C. M. and Brimblecombe, P. 2008. Past and Future Patterns of Historic Stone Buildings. *Materiales de Construccion*. 58 (289-90): 143-160

İstanbul Büyükşehir Belediyesi.2010. http://sehirrehberi.ibb.gov.tr .(accessed July 22, 2010)

Lefévre, R. A. and Ausset, P. Atmospheric Pollution and Building Materials: Stone and Glass. Ed. Siegesmund, S., Weiss, T. and Vollbrecht, A. 2002. *Natural Stone, Weathering Phenomena, Conservation Strategies and Case Studies*. The Geological Society. London. Special Publication no. 205: 329-345

Montana, G., Randazzo, L., Oddo, I. A. and Valenza, M. 2008. The Growth of 'Black Crusts' on Calcareous Stones in Palermo (Sicily): a First Appraisal of Anthropogenic and Natural Sulphur Sources. *Environmental Geology*. 56: 367-380

Montoya, C., Lanas, J., Arandigoyen, M., Garcia Casado, P. J. and Alvarez, J. I. 2004. Mineralogical, Chemical and Thermal Characterisations of Ancient Mortars of the Church of Santa Maria de Irache Monastery (Navarra, Spain). *Materials and Structures/ Matériaux et Costructions*. 37: 433-439

Moroni, B., Pitzurra, L. and Poli, G. 2004. Microbial Growth and air Pollutants in the Corrosion of Carbonate Building Stone: Results of Laboratory and Outdoor Experimental Tests. *Enviromental Geology*. 46 (3-4): 436-447

Nord, A. G. and Holenyi, K. 1999. Sulphur Deposition and Damage on Limestone and Sandstone in Stockholm City Buildings. Springer Netherlands. *Water Air and Soil Pollution.* 109: 147-162

Nuhoğlu, Y., Oğuz, E., Uslu, H., Ozbek, A., Ipekoğlu, B., Ocak, I. and Hasenekoğlu, İ. 2006. The Accelerating effects of the Microorganisms on Biodeterioration of Stone Monuments Under Air Pollution and Continental-cold Climatic Conditions in Erzurum, Turkey. *Science of the Total Environment*. 364 (1-3): 272-283

Ocak, Y., Sofuoğlu, A., Tıhmınlıoğlu, F. and Böke, H. 2009. Protection of Marble Surfaces by Using Biodegradable Polymers as Coating Agent. *Progress in Organic Coatings*. 66: 213-220

Pitzurra, L., Moroni, B., Nocentini, A., Sbaraglia, G., Poli, G. and Bistoni, F. 2003. Microbial Growth and Air Pollution in Carbonate Rock Weathering. *International Biodeterioration & Biodegradation*. 52 (2): 63-68

Rona, Z. 1997. "Art Nouveau", *Eczacıbaşı Sanat Ansiklopedisi*. YEM Yayın. İstanbul. Vol. 1 pp. 141-142

Screpanti, A. and Alessdandra, D. M. 2009. Corrosion on Cultural Heritage Buildings in Italy: A Role for Ozone. *Environmental Pollution*. 157 (5): 1513-1520

Skoulikidis, T.N. and Beloyannis, N. 1984. Inversion of Marble Sulfation – Reconversion of Gypsum Films into Calcite on the Surfaces of Monuments and Statues. *Studies in Conservation*. 29: 1733-1743

Striegel, M.F., Guin, E.B., Hallett, K., Sandoval, D., Swingle, R., Knox, K., Best, F. and Fornea, S. 2003. Air Pollution, Coatings and Cultural Resources. *Progress in Organic Coatings*. 48: 281-288

Thompson, M., Shelley, J., Compton, R.G. and Viles, H.A. 2003. Polymer Coatings to Passivate Calcite from Acid Attack: Polyacrylic Acid and Polyacrylonitrile. *Jounal of Colloidal Interface Science*. 260: 204-210

Török, A. 1997. Deterioration of limestone buildings as a result of air pollution, examples from Budapest. Ed. Marinos, P.G., Koukis, G.C., Tsiambaos, G.C. and Stournaras, G.C. *Engineering Geology and the Environment*. A.A. Balkema, Rotterdam.

Török, A. 2004. Comparison of the Process of Decay of Two Limestone in a Polluted Urban Environment. Ed. Searle, D. and Mitchell, D. *Stone Deterioration in Polluted Environments (Land Construction and Management Series, Vol.3)*. Science Publisher. U.S.

Török, A. 2007. Characteristics and Morphology of Weathering Crusts on Porous Limestone the Role of Climate and Air Pollution. In *Preservation of Natural Stone and Rock Weathering*. Proceedings and Monographs in Engineering. *Water and Earth Sciences* :61-66

Török, A. 2008. Black Crusts on Travertine: Factors Controlling Development and Stability. *Environmental Geology*. 56 (3-4): 583-594

Tuğrul, A., Zarif, İ. H. and Gürpınar, O. 1998. Deterioration of Limestone at Şehzade Mehmed Mosque and Other Monuments due to Action of Air Pollutants in İstanbul, Turkey. Eight International Congress International Assaciation. *Engineering Geology and the Environment Proceedings*. 1-5: 2923-2930

Tuğrul, A. and Zarif, İ. H. 1999. Research on Limestone Decay in a Polluting Environment, İstanbul – Turkey. *Environmental Geology*. 38 (2): 149-158

Venice Charter. 2009. http://www.icomos.org/venice_charter.html . (accessed September 24, 2009).

Webb, A. H., Bawden R. J., Busby, A. K. and Hopkins, J. N. 1992. Studies on the Effects of Air Pollution on Limestone Degradation in Great Britain. *Atmospheric Environment Part B. Urban Atmosphere*. 26 (2): 165-181